

We are IntechOpen, the world's leading publisher of Open Access books Built by scientists, for scientists

6,900

Open access books available

186,000

International authors and editors

200M

Downloads

Our authors are among the

154

Countries delivered to

TOP 1%

most cited scientists

12.2%

Contributors from top 500 universities



WEB OF SCIENCE™

Selection of our books indexed in the Book Citation Index
in Web of Science™ Core Collection (BKCI)

Interested in publishing with us?
Contact book.department@intechopen.com

Numbers displayed above are based on latest data collected.
For more information visit www.intechopen.com



Shock-Wave-Compaction (SWC) of Al/CNT Two Phase Systems

Noé Alba-Baena¹, Wayne Salas² and Lawrence E. Murr³

¹*Universidad Autónoma de Ciudad Juárez, México*

²*Tinker Air Force Base, USA*

³*University of Texas at El Paso, USA*

1. Introduction

The scientific investigation and applied research on composite materials can date back to the 1940's (Schwartz, 1997) with the advantages behind the development of metal matrix composites (MMCs) being the capability to combine phases providing a potential for tailoring material properties to meet specific and challenging requirements. Composites offer an approach for producing "designer" materials used to provide specific types of material behavior, such as their improved strength and stiffness (Ward et al, 1996), outstanding corrosion resistance (Shimizu et al, 1995), friction resistance (Akbulut et al, 1998) and wear resistance (Wang et al, 1996), high electrical and thermal conductivity (Koráb et al, 2002), and high temperature mechanical behavior (Tjong & Ma, 1997). Currently, metal matrix composites can be classified by reinforcement component into fibers (continuous or discontinuous), whiskers, particulates, or wires. These reinforcements have been placed in matrices of aluminum, magnesium, copper, titanium, nickel, nickel-based superalloys, and various alloys of iron. However the aluminum matrix alloy composites are those that have become an industry standard because they offer the advantage of lower cost when compared to most other MMCs. Aluminum based composites also offer the added benefits of excellent thermal conductivity, high shear strength, excellent abrasion resistance, high-temperature operation, and the ability to be formed and treated on conventional equipment (Schwartz, 1997). Conventional metal matrix composites have been manufactured through several various processing methods. These processes can generally be categorized into four general groups: solid-state processes, liquid-state processes, deposition processes and in-situ processes. Solid-state and liquid-state processes are the two most widely used and developed methods (Everett & Arsenault, 1991). Particulate composites reinforced with micron-sized particles of various materials are perhaps the most widely utilized composites in everyday materials. Particles are typically added to enhance the matrix elastic modulus and yield strength. By scaling the particle size down to the nanometer scale, it has been shown that novel material properties can be obtained (Thostenson et al, 2001).

The nanocomposite materials, especially those using carbon nanotubes as reinforcement, have recently garnered great interest and tremendous growth from scientists and engineers in the research field (Salvetat-Delmotte & Rubio, 2002). This spurt of interest in nanocomposites stems from the unprecedented flexibility and improvements in physical properties that may be attained by using building blocks with the dimensions in the nanoscale range. It may be possible to design and create new tailored composites by using nanosize building blocks of heterogeneous dispersed phases. Thus, the materials designed from them can be multifunctional because the constituents of a nanocomposite have different structures and compositions and therefore different properties. In many cases, the interesting range may be located near the transition where properties are changing from the molecular to bulk-like, a size range in which properties can be manipulated in a positive way in order to design a material for a particular application (Oelhafen & Schuller, 2005).

It is true that nanometric sized particles help to achieve improved mechanical properties (Sahin & Acilar, 2003; Raming et al, 2004 and Lan et al, 2004) depending basically in the type of second phase nanomaterial and the dispersion strengthening due to the particle distribution and volume fraction variation. But currently much attention has been given to the possibilities of incorporating carbon nanotubes (CNTs) as the nano reinforcement in a matrix or as a second phase in two phase systems. This is not only due to the well known remarkable mechanical properties of CNTs but also in the belief that they may very well be the ultimate fiber reinforcement based on their high aspect ratio and defect-free structure. Application and innovations will take advantage of the special properties based on carbon nanotubes including electrical, mechanical, and other unique properties. The construction of composites with extraordinary properties will be related to the multifunctional materials that can be developed. Most investigators who are developing new composite materials with nanotubes work with nanotube concentrations below 10%wt due to limited availability of nanotubes. With continued developments in the synthesis and production of carbon nanotubes, new possibilities in the field of composite materials based on carbon nanotubes are emerging (Meyyappan, 2004). Although much of the present research is in the area of polymer composites, efforts in metal and ceramic matrix composites are also of interest. Studies, especially in polymers, focus on dispersion, untangling, alignment, bonding, molecular distribution, and retention of nanotube properties. Carbon nanotubes are theoretically one of the strongest and stiffest materials with a calculated tensile strength of ~200 gigaPascal and modulus of more than 1-4 teraPascal for a single walled nanotube (SWNT) (Dresselhaus et al, 2001). If the mechanical properties of SWNT could be effectively incorporated into a matrix, composites with lightweight, exceptional strength and stiffness can be achieved. It is expected that nanotube composites will be used as a replacement for existing materials where properties superior to conventional composites are achieved and to create materials for applications where composites traditionally have not been used before. Therefore, one of the most important outcomes from current nanocomposite research will be knowledge that is gained about preparing materials for the development of the nanocomposites in the future. The applications for nano-metal matrix composites (NMCs) are nanowires, lightweight structures, electronic materials for avionics, wear coatings, novel magnetic and super conducting systems and new multifunctional metals (Meyyappan, 2004 and Ajayan et al, 2003).

In order to tailor these bulk nano-based (NMCs), actual approaches have used conventional powder metallurgy with adapted techniques (as ultrasonic mixing and wetting preparation), where matrices of aluminum, copper, magnesium and silver have been used. Benefits from this approach arise based in the process work temperature that is below the melting temperature of the metals (melting temperature for Al is 660°C) (Ajayan et al, 2003). Powder metallurgy routes using powders and in some cases extrusion have produced an Al metal matrix composite, copper electrodes, and macroscopic composite wires (where extrusion was used). However, the resultant NMCs has exhibited modest improvement of its properties as compared to those characteristic of traditional metal-matrix composites (MMCs) (Salvetat-Delmotte & Rubio, 2002). Such performance can be mainly attributed to the tendency of the nanomaterials and specially the carbon nanotube (CNT) material to variously agglomerate and cluster. This leads to difficulties in the dispersion of the CNTs in the metal matrix, as well as poor wetting, or related interfacial phenomena and integrity issues. The results achieved by using high-intensity ultrasonic waves with strong micro-scale transient cavitations and acoustic streaming to successfully introduce, distribute and disperse nanoparticles into Mg alloy melts and Al matrices, thus making the production of cast high-performance nano-sized particles reinforced matrix composite promising (Rohatgi et al, 2008). In order to take full advantage of the exceptional stiffness, strength and resilience of carbon nanotubes requires a uniform dispersion of CNTs in the metal matrix. This dispersion will ensure a strong interface bonding between the CNTs and the surrounding matrix which provides effective stress transfer, as well as avoids intra-tube sliding between concentric walls within MWCNTs and intra-bundles sliding within SWCNT ropes. Efforts are in progress to overcome these difficulties. Recently, Zhong et al also studied nanocrystalline Al matrix reinforced with SWCNTs that were successfully fabricated by cold-consolidation and hot consolidation (Zhong et al, 2003). Their procedure of mixing nano-Al particles and SWNTs results in a homogeneous dispersion of SWNTs and shows that the ultrasonic energy could overcome the van der Waals force between SWNT bundles and between nano-Al particles. From this work one can infer that when used as the matrix of composites, nano-materials can be more compatible with CNTs than traditional matrices of metal, ceramic matrix, and polymer. The reported hardness of the SWNT/nano-Al composites reached a peak value of 2.89 GPa, which shows that SWNTs are a promising reinforcement for some matrices.

Conventional process seems to inhibit the diffusion of CNTs across and along the matrix grain surfaces. Sintering cannot proceed without damaging the CNTs or removing them from the liquid state matrix or if the diffusion is achieved CNTs are mostly located at grain boundaries of the matrix and are insignificant in improving material performance (Cha et al, 2005). The most important processing issue is the interfacial strength between the CNTs and the matrix. In the case of successful CNT/polymer nanocomposites, the interfacial strength between the CNTs and the polymer matrix is strong because they interact at the molecular level. In the case of CNT/metal nanocomposites, however, the interfacial strength cannot be expected to be high because the CNTs and the matrix are merely blended. In their research, Cha et al (2005) uses a novel molecular mixing approach in order to produce a metal/CNT composite rather than a two-phase system. As result, it was reported that CNTs are shown not merely lying at grain boundaries but diffusing across grain boundaries. Some work as been done on one-dimensional nanoscale composites prepared by coating the carbon

nanotubes, by electroless plating, with other materials such as Co and Ni (Chen et al, 2000 and 2003). Such studies address in part the problem of interfacial adhesion between the nanotubes and the metal matrix; it is thought that high strength adhesion between nanotubes and the metal matrix can be achieved by coating the nanotubes with metallic material. Probst (2005) et al states the possibility that carbon nanotubes may not be used as a reinforcement phase without prior treatment. Probst reports that CNTs can be wetted only by liquids, or by molten metals with low surface tension at a cut-off limit lying between 100 and 200 mN/m (Jordan J. L. et al, 2001). This explains why most metals such as aluminum (surface tension of 865 mN/m), copper (1270 mN/m) or iron (1700 mN/m) are not able to wet the surface of nanotubes and achieve high interfacial adhesion. In their work, Lijie et al focuses on the interfacial reaction between CNTs and aluminum in Al/CNT composite films that were fabricated by sputtering pure Al on the surface of aligned multi-walled CNT arrays (Lijie et al, 2006). After heat treating, annealed samples show that, at various temperatures, aluminum carbide (Al_4C_3) was formed at the interface between the Al and CNT layers at defect sites and at open ends of CNTs. More recently novel approaches and fabrication processes have been reported. Bakshi et al (2008) successfully synthesized aluminum composites reinforced with CNTs by cold spraying of a blended powder. They reported an elastic modulus ranging between 40-120 GPa and attributed such variation mainly to the exhibited porosity and the agglomeration of CNTs. Laha et al (2009) used plasma spray forming (PSF) to fabricate Al-Si/MWCNTs composites measuring up to a 78% increase in the elastic modulus of the composite; also attributing such variation to the composite's porosity and the CNTs agglomerations. Lim et al (2009) also reported the production of aluminum alloy reinforced with multi-walled carbon nanotubes composite by using a friction stir processing where images and conclusions show the agglomeration of CNTs.

1.1 Two phase systems

Therefore the fabrication of two phase systems (TPS) that involves the incorporation of a second phase or reinforcer; such as particles, platelets, whiskers and fibers, to a continuous phase are differentiated primarily by the interaction between the grains (aluminum grains in this study) and the nanoparticles (carbon nanotube aggregate mixture for this study). The differences between the systems that involve more than one phase are related, in general, to the fabrication process either in the solid or liquid phases, therefore it is necessary to define a TPS as opposed to a MMC. According to Torquato (2002), a TPS is a heterogeneous material composed of domains of different materials (phases) such as composites or the same material in different states such as a polycrystal. Kennedy et al (2001) considers a two-phase system as a system where the continuous phase network (large grains) is surrounded by the second phase and the phases are interdispersed and uniformly inter-twinned with each other. This definition better expresses the concept of a TPS as used in this chapter. While a continuous phase is described for both; the difference should lie in the effectiveness of traditionally known strengthening mechanisms. The two-phase system has a different set of properties and microstructures when compared to the MMC. TPSs and MMCs can now be related to their fabrication processes: MMCs are those fabricated by liquid stage processes such as mixing the matrix grains and the particle grains by using ultrasonic dispersion, mechanical stirring and others. TPS are considered as resultant of the use of solid state processes as powder metallurgy (P/M), high temperature synthesis (SHS),

mechanical mixing (MM), hot pressing (HP) and shock wave compaction (SWC) (Kennedy et al, 2001). In this case surface phenomena tend to dominate fine powders, primarily due to their high surface-to-volume ratio and in such cases van der Waals, electrostatic, and surface tension forces often have dominating effects on properties. Handling these particles is extremely difficult, and high aspect ratios (as in fine whiskers and SWCNT) further complicate the handling problem. There are cases when systems using CNTs were fabricated and reported in the literature as MMCs. In these cases the agglomeration of CNT aggregate in the nanometric regime is much larger than the molecular dimensions, so that the agglomerate may possess properties in the macroscopic level. These MMCs may be classified as heterogeneous two phase or two component systems with heterogeneous materials ranging from dispersions with varying degrees of clustering to complex interpenetrating connected multiphases. An example of a two phase system is described by Kim et al. where the microstructure of CNT/Cu nanocomposites show that the carbon nanotubes are not homogeneously distributed in Cu matrix, but the carbon nanotubes are densely distributed in localized regions (Kim et al., 2006). The microstructure of CNT/Cu nanocomposites consists of two regions including a CNT/Cu composite region, where most CNTs are distributed, and a CNT free Cu matrix region (continuous phase). Ajayan et al (2003) consider that the relationship between particles and grains can be divided in four grain/particle types shown in Figure 1.

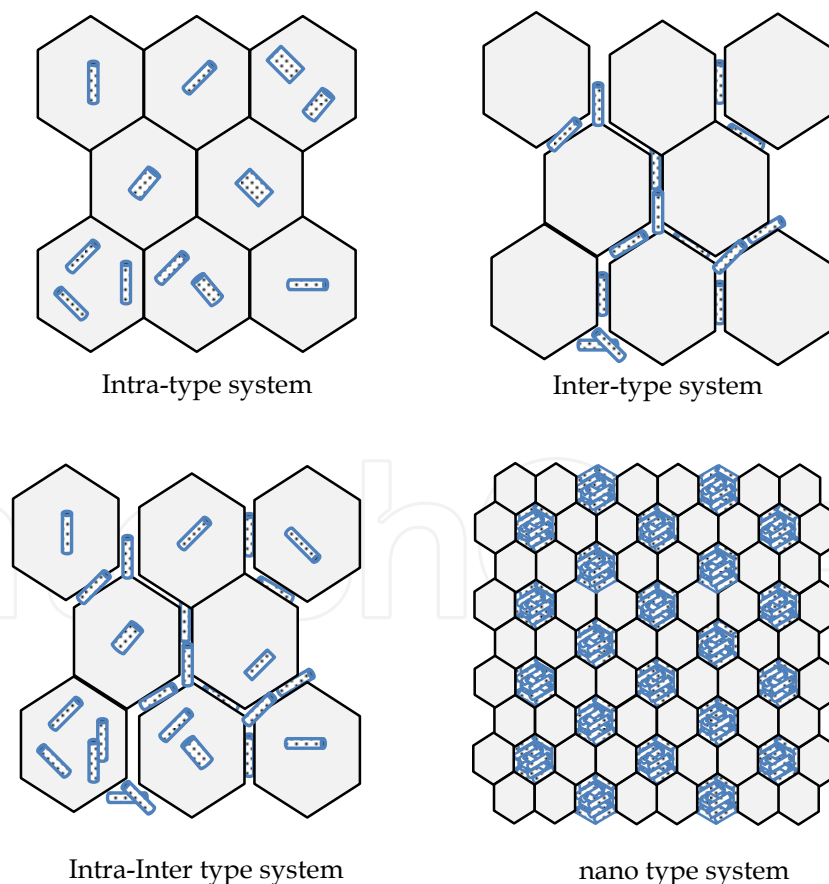


Fig. 1. Representation of different systems that can be obtained by using nanoparticles (adapted from Ajayan et al, 2003).

The first to appear is the intragranular type of interaction. This intra-type system is often addressed as the pure MMC, which results from the inclusion of the nanoparticles or CNT (for our purposes) in the grains usually during a liquid state process. For this system the grains form a matrix in which the CNTs or reinforcers are included, i. e. CNTs affect the matrix by generating internal dislocations which increase the tensile and hardness properties. The inter-type interaction shown in Figure 1 consists of the CNTs sitting along the grain boundaries of the continuous phase affecting the grain to grain bonding of the system. In this intergranular type system the grain/CNT relationship remains constant with the grains remaining without inclusions. This system is based in the volume fraction of the reinforcement with the addition of CNTs reaching a saturation point. An independent phase forms after the saturation point of the CNTs which agglomerate and form at the grain boundaries of the continuous phase. The resultant system from the interaction of the particle agglomerations and the grains can be address as a two-phase system. A combination of previously mentioned systems (inter-intra type) is also shown in Figure 1; the microstructural representation of the combination system of intragranular and intergranular usually results from the fabrication by stir casting processes which can be considered an imperfect MMC. Examples of this kind of systems have been achieved by means of traditional P/M processes where attempts to fabricate CNT/metal composites with homogeneously dispersed CNTs have been attained. Resultant systems show strong interaction of CNTs in powder form (due to Van der Waals forces) and CNTs agglomerate rather than homogeneously disperse. In general, if the CNT/metal nanocomposites are manufactured by conventional processes (liquid or solid); most of the CNTs are located on the surfaces of the metal particles as agglomerates and dispersed forms. Finally, a nano/nano type system is represented in Figure 1, such system is what is hoped to be achieved in a true nano-scale two-phase system where either the nanoparticles (or CNTs) and the principal phase lie in the nanoregime. Still, the ideal metal/CNTs composite does not fit the previous descriptions and has not yet been achieved by experimental processes but the Figure 2 schematic represents a proposed case for a metal/nanotube composites. Here CNTs are shown not merely lying at grain boundaries agglomerating or immersed in the matrix grain, but nanotubes are shown diffusing across grain boundaries in an ideal fashion.

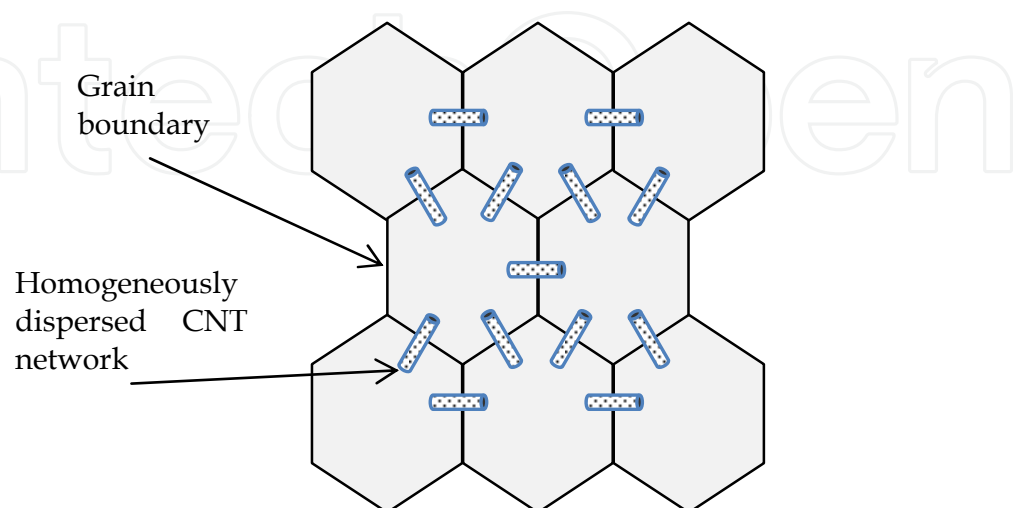


Fig. 2. Ideal microstructure of a Metal/CNT composite (Adapted from Wang et al, 1996)

2. Shockwave consolidation of powders

In an extensive report, Meyers et al (2006) reviewed and summarized the literature on the mechanical properties of nanocrystalline materials. The report defines the most important synthesis methods for powder densification (including SWC) and a number of aspects of mechanical behavior showing the potential benefits and drawbacks in the fabrication of nanocomposites. While there have been several recent examples of carbon nanotube/metal composite systems fabrication (Rao et al, 2006 and Kowbel, 2005) utilizing conventional powder metallurgy (P/M) routes, there has been no evidence of any significant improvement in properties that characterize traditional MMCs (Lan et al, 2004 and Yang et al, 2004). This is due in part to the CNT material agglomerating, and the difficulty to disperse the CNTs in the metal matrix as a consequence of poor wetting, related interfacial phenomena, or integrity issues. Also of concern is high temperature exposure required by the processing of composites by the conventional mechanical stirring, ultrasonic dispersion and powder metallurgy.

As a method to avoid the formation of intermetallic compounds and where the grain size is to be preserved, an alternative way to consolidate composites is by dynamic compaction (or SWC) (SivaKumar et al, 2001). The densification of powders by shock waves has gained revived interest as a technique for the consolidation of TPS, amorphous and nano-crystalline powders, e.g. for magnetic applications. This revised interest stems in part because TPS's are systems where microstructural and mechanical properties depend on the connectivity between a continuous-phase surrounded by an interdispersed second-phase, and also because the SWC process has a very high 'dynamic' energy rate and the energy is mainly deposited on the grain boundaries thus bulk heating is very much limited. Moreover, SWC characteristics make it even more suitable for the densification of composites of otherwise incompatible materials, such as polymeric and ceramic powders, which may lead to some distinct industrial applications (Yang et al, 2004). As an example, the full densification of metallic-ceramic mixtures of Al (30% volume fraction) and B₄C has been reported, where the major drawback of this technique is the occurrence of cracks, which can be avoided when the starting materials show some plastic behavior.

For the purposes of this chapter SWC is reviewed in extend because of its possibility as an alternative for the densification and synthesis of nano-sized composites (Withers, 2005), and similarly, to consolidate nano-two-phase systems (Wang X. et al, 2004). Prummer (2001) has reviewed SWC from its origins, which now spans more than four decades. Over this time, shock-wave consolidation has been used for the densification and synthesis of ceramic compounds based on powder mixing (Dorst et al, 1997 and Jordan & Thadani, 2001), and similarly, to consolidate two-phase systems (Kennedy et al, 2001). This consolidation process has been shown to be a suitable option to produce 100% dense nanocrystalline Al₂O₃ (Torralba et al, 2003), along with a variety of ceramics and other nano-materials. SWC has also proven to be effective in the synthesis of materials (diamond for example) (Yang et al, 2004; Wang L et al, 2004; and Sherif El-Eskandarany, 1998). In addition to the different benefits of SWC introduced above, SWC is the technique lending itself best to industrial production. The costs are low therefore the process lends itself to scale up without major problems. Since the 50s many reports have been presented (Rice et al, 1958; Kimura, 1963 and Kawala et al, 1974) and recently have been published on shock consolidation of

powders (Prummer & Ziegler, 1985; Thadani, 1988; Glade et al, 1995). However, publications on the explosive compaction of CNT aggregate material are limited and there is very little information available on processing of metal-matrix nanocomposites by explosive compaction. Salas et al (2007) have employed SWC as an approach to creating a two-phase monolith from mixtures of varying volume fractions of multiwalled carbon nanotube (MWCNT) aggregates with micron-size ($\sim 150 \mu\text{m}$) aluminum powder. These two-phase systems were of special interest because the MWCNT aggregates were obtained from as-manufactured mixtures of tubes and various sizes of multi-concentric fullerenes (with diameters ranging from ~ 2 to 40 nm) it was not clear whether these aggregates could themselves be consolidated into a contiguous phase region, and whether this regime would be bonded, monolithically, to the consolidated aluminum particle regime.

2.1 SWC process

During SWC the densification of the powders is accomplished by the passage of a strong shock wave generated upon the impact of a flyer plate onto the green compact (target powder). Shock pressures of 3-15 GPa or higher are commonly used and a typical shock rise time is of the order of 100 ns during which the densification process is complete (Kennedy et al, 2001). The physical phenomena of such a dynamic consolidation process at the particle level are very complex and remain poorly understood.

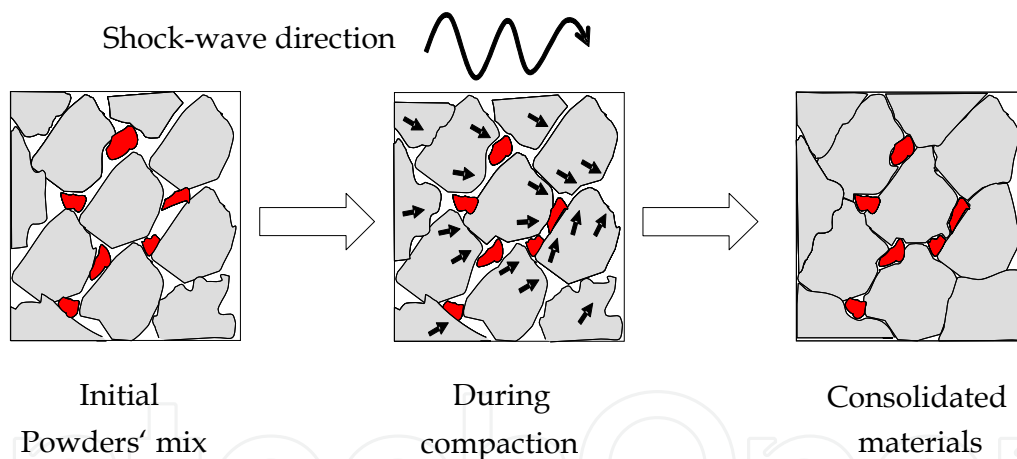


Fig. 3. Schematic view of a TPS shock-consolidation process to illustrate the shock-wave effect in the powder material grains.

However, as shown in Figure 3 and explained by Tong et al (1995), during shock-wave densification, energy is mainly deposited near the particle surfaces and the resulting heating produces softening and even melting of the particle surfaces that solidify rapidly via heat conduction into the interior of the particles before release of shock pressure. First the reduction of pores takes place through the sliding and rearrangement of particles. Then, the densification takes place by surface plastic deformation (at particle contacts) over small areas where initially free surfaces become areas of contact and the localized energy deposition at interparticle surfaces has been attributed to local plastic deformation and some frictional sliding that contributes largely to the particle-particle bonding (Tong et al, 1995) as

illustrated by the single phase consolidated material images from Figure 4. Here an arrangement of tungsten rods were implosively consolidated as two dimensional grains, also one can observe the collapsed pores and the deformation of the grains (rods) after plastic sliding. Finally, 3rd image of Figure 4 illustrates the consolidation of TPS where the second phase particles are all locked up and surrounded by the solid primary phase through the densification that takes place at the same time of the pores collapse.

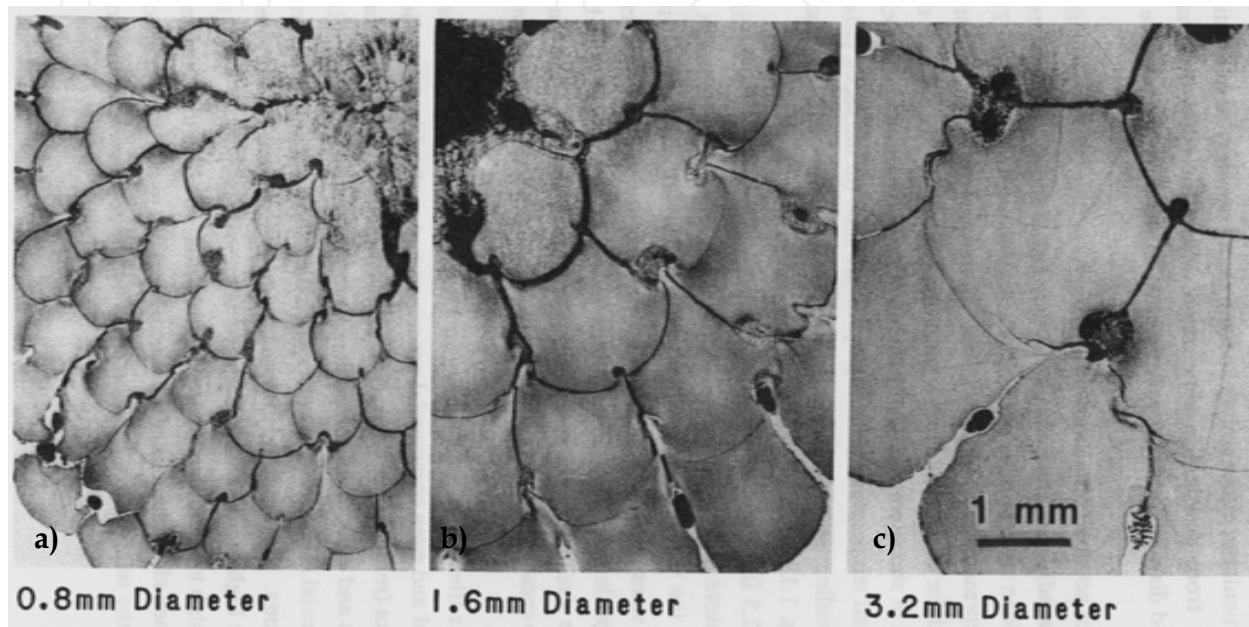


Fig. 4. Sequence showing an arrangement of tungsten rods representing a two dimensional consolidation after SWC process (from Murr, 1998).

2.2 Type of SWC methods

Murr (1998) categorizes the shock-wave consolidation processes into two major groups; the direct and indirect methods or consolidation techniques. The main difference between the two methods is the way that the pressure is applied to the sample or materials mixture. The direct methods require minimum tooling, are relatively inexpensive, and do not have geometrical limitations. The indirect methods are usually more expensive and employ fixturing, tooling, or a liquid transmitting media to achieve the same uniformity in the final product densities. The single stage or three-capsule gas-guns that were used to synthesize β - C_3N_4 (Collins et al, 2001) and intermetallics such as Ti_5Si_3 (Counihan et al, 1999) alloy and NiAl (Chen et al, 1999) and to successfully consolidate magnetic nanocomposites ($Pr_2Fe_{14}B/\alpha$ -Fe) (Jin et al, 2004) are elaborate and reliable. Here the experiments are performed using guided projectiles that impact on flyer plates to incident one-dimensional shock. Shock-wave consolidation direct methods are basically two and can be exemplified with the cylindrical and plate configurations that are the most representative of these experimental setups. Plate configured experiment set ups provide higher pressures than explosives in direct contact with the material (Meyers and Wang, 1988). A well used plate configuration is the Sawaoka experimental variation. This configuration along with the Sandia calibrated shock recovery fixtures are intended to control and make reproducible the high pressure compression conditions (Murr, 1998). Plate configured experiment set ups

provide higher pressures than explosives in direct contact with the material (Meyers and Wang, 1988). Here the densification of the powders is accomplished by the passage of a strong shock wave pressures generated upon the impact of a flyer onto the green compact (or packed powder) (Tong et al, 1995). Many reports on successful consolidation of different powder mixtures by using this set up can be recalled: Ti/SiCp (Tong et al, 1995), Al-SiC (SivaKumar et al, 2001), Al-Li-X alloys (Murr, 1998), carbon fiber aluminum composites (Raghundan et al, 2003), Mo-Si powder mixtures (Vandersall and Thadani, 2001) and the synthesis of diamond from fullerenes (Epanchintsev et al, 1997). Common tube configurations use single and double tube setups (Stuivinga et al, 1999). Single tube configuration is a simple design, where the green compacted powders are placed in a thin walled metal container (or pipe) encapsulated by the use of solid metal end plugs (see Figure 5) filled with the chosen explosive material and an electrical activated detonation, a fast explosive layer, is initiated at the top of the set up.

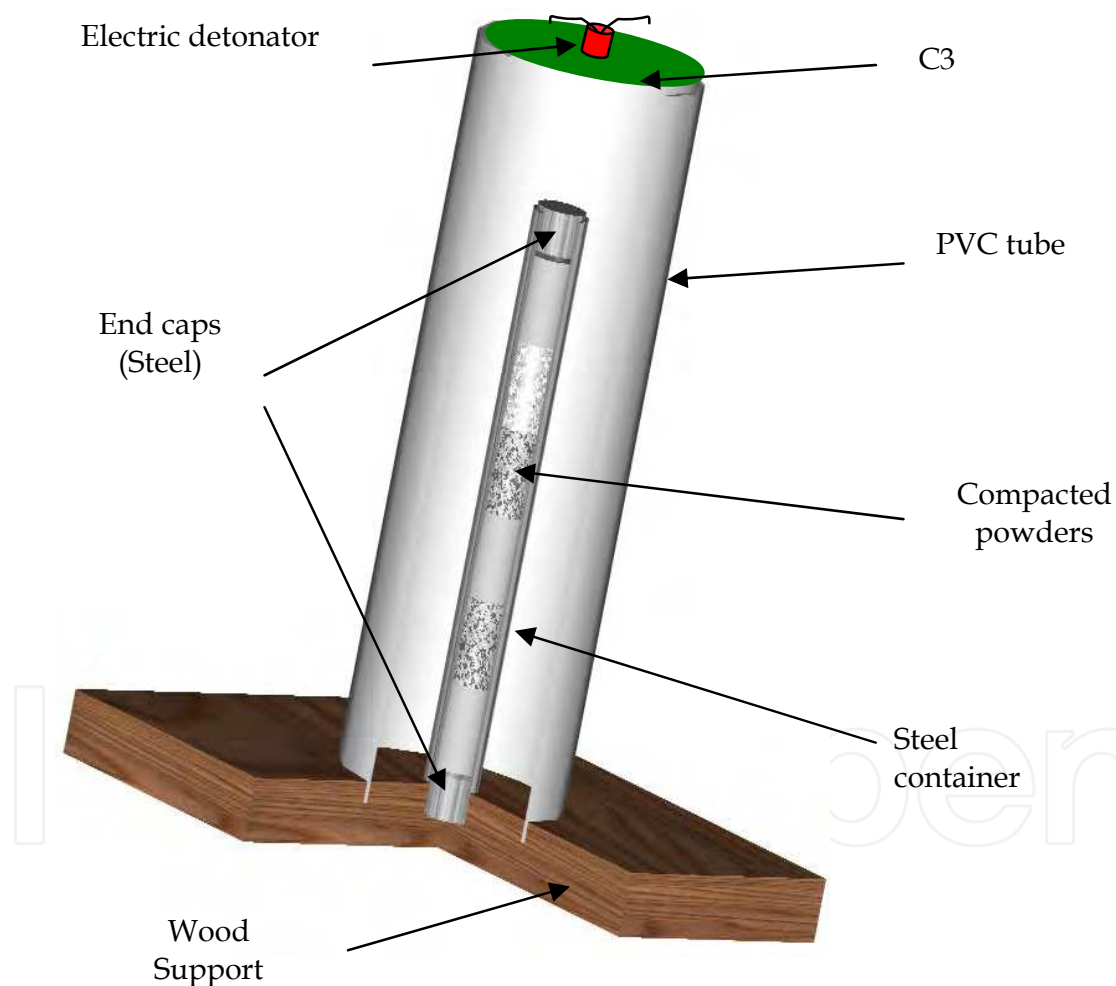


Fig. 5. Basic components of a simple cylindrical compaction set up.

The detonation wave in the explosive propagates parallel to the cylinder axis, generating oblique shock-waves to converge towards the central axis of the cylinder and if the energy applied is excessive, radial cracks and/or a mach stem can occur in the consolidation sample. Many researchers have employed explosive compaction set up, for example, to

densify aluminum and Al-SiCp composite powders (SivaKumar et al, 1996), for dual phase nanocomposite systems of Y_2O_3 -doped with ZrO_2 and RuO_2 (Raming et al, 2004) and more recently Al-Pb nanocomposites (Csanady et al, 2006) and nanocrystalline alumina powder (Weimar & Prummer, 2001). The double tube set up is, conceptually, analogous to the use of a flyer plate to generate high pressures in plane-wave assemblies (Meyers and Wang, 1988). The basic difference with the conventional explosive consolidation systems is that a flyer tube is placed co-axially with the container tube. The experimental setup consists of two co-axial tubes, the external one being accelerated inwards and impacting the internal tube, that contains the powder. The basic experimental set-up is similar to the described single tube set up. The explosive is placed in the cylinder, at the center of which is the assembly containing the powder (Murr, 1998). The explosive charge is detonated at the top; a detonation sheet (detasheet) booster is used to create a more uniform detonation front. This approach ensures high shock pressures while retaining a low detonation velocity which minimizes cracking and Mach stem formation. An improvement was made by Meyers and Wang (1988) proposing a variation in the central axis of the container by placing a solid rod. Substantial improvements in the quality of consolidates was obtained by using this technique, where the pressures generated in the powder are several times higher than the one for the single-tube geometry, for the same quantity and type of explosive. There has been reported significant improvement in consolidation quality of nickel-based superalloys, titanium alloys, Al-Li alloys (Kennedy et al, 2001; Kim et al, 2006). There are reports on the consolidation of superconducting YBCO (Mamalis et al, 2001), the consolidation of synthetic diamond (Deribas et al, 2001), the synthesis of intermetallic compounds such as TiAl (Prummer and Kochsler, 2001) and the densification of B_4C (Stuivinga et al, 1996) for example.

3. Al/CNT Two-Phase Systems Fabrication

The characterization of Al/2%CNT and Al/5%CNTs systems based on a previous report (Salas et al, 2007) is shown here in order to describe the fabrication of TPS by using CNTs and SWC to consolidate materials. Irregular (spherical) and small aggregates of aluminum powder, with an average primary particle size of $\sim 150 \mu m$, served as a base phase to which commercial aggregates of multiwalled carbon nanotubes and other assorted multi-concentric fullerenes were added in two different volume fractions (2 and 5%) for mixtures that were mechanically mixed. The CNTs percentage is decided upon from previous studies which indicate percentages of 10% and above result in a significant decrease in measured mechanical properties (Xu et al, 1999 and Feng et al, 2005) while percentages below 5% have been used in previous studies by different fabrication methods with several reported increases in mechanical properties. These mixtures, along with the pure aluminum base powder, were placed in 3.2 cm inside diameter steel tubes with one end containing a welded plug, as previously shown in Figure 5. The aluminum powder was first added to the tube and filled to accommodate a very close fitting steel mandrel which was inserted into the tube with a 4536 kg force to produce a green compact of $\sim 70\%$ density for a 5.08 cm aluminum test cylinder. To this initial compacted aluminum base powder the MWCNT aggregate powder/aluminum powder mixtures were added to a calculated height to produce a 5.08 cm test cylinder when compacted to $\sim 70\%$ density. These Al/2 and 5% MWCNT were alternated along with the pure aluminum powder base as compacted $\sim 75\%$

and other two-phase powder mixtures to create a series of 6 compacted-powder sections within the steel tube. The open end was then sealed with a welded steel plug and this steel-enclosed assembly was then inserted into a wooden base and surrounded by a 15.25 cm diameter PVC tube 7.6 cm taller than the steel test cylinder, also shown in Figure 5. This PVC container was filled with ammonium nitrate-fuel oil (ANFO) and a thin sheet of detasheet with a central detonator added to the top of the ANFO-filled PVC tube to initiate the reaction. The reaction is given by

$$P=(\rho_0 D^2)/2 \quad (1)$$

using an ANFO density (ρ_0) of ~1.2 g/cc and detonation velocity (D) ~3500 m/s the initial pressure was calculated (as described by Meyers and Wang, 1988) to be ~7 GPa. These arrangements or assemblies were placed on sand bags, which allowed the explosively consolidated steel tubes to be easily retrieved from the ground after detonation on the facilities of the New Mexico Tech EMRTC (Energetic Materials Research & Testing Center) installations. The recovered TPS characterization was performed on machined sections from the compacted recovery tubes. To help preserve the integrity of the microstructure of the materials a wire electric discharge machining (WEDM) was employed to cut segments for the preparation of light microscopy, SEM, (and FESEM), TEM, and hardness testing. The WEDM used is a 5 movement axis RoboFil 310 wire-electrical discharge machine (Charmilles Technologies) with a CuZn25 electrode wire in a diameter of 0.25 mm that proves to be a reliable technology for the purpose of cutting test specimens and samples. Along with the sections that contained the carbon nanotubes second phase, the consolidated aluminum was of interest as reference or control sample. Sections to be used for light metallography and SEM imaging were first ground using grit papers from 400 grit SiC down to 1200 grit SiC (using an Ecomet 6- Buehler variable speed grinder- polisher at 200 rpm), and then polished using a non-crystallizing colloidal silica suspension to a 1 micron finish, with a soap and water mixture (1:200) as the primary lubricant. For etching, a variation of Keller's reagent was used with a composition of 100 mL of water, 6 mL of nitric acid, 6 mL of hydrochloric acid, and 6 mL of hydrofluoric acid. The imaging was performed in a Reichert MEF4 A/M (Leica, Corp) light microscope and the same samples were used for SEM and field-emission SEM (FESEM, Hitachi S-4800) imaging. The TEM specimens were prepared from machined sections of the Al/MWCNT systems along with the aluminum monolith that were reduced by grinding to a thickness less than 0.5 mm, then 3 mm discs were punched from these thin-slice sections which were perpendicular to the compaction tube vertical directions (Figure 5). Electropolishing was done with a Tenupol-5 dual jet electropolisher using an electrolyte with a composition of 250 mL of nitric acid and 850 mL of methanol at -15°C. TEM imaging was performed using a Hitachi H-8000 analytical transmission electron microscope operating at 200 kV accelerating potential. An INSTRON Rockwell hardness tester, 2000 series was used to take Rockwell (E-scale) hardness reading profiles of the obtained systems, and the consolidated aluminum, for comparison. Vickers hardness measurements were also made using a Shimadzu microhardness tester employing a 25gf (0.25 N) load. Micro-tensile testing was performed using samples cut parallel to the consolidation axis and proportional to 60% of the D-638, type V ASTM standard specifications (with a gauge length of 9 mm) and an INSTRON tensile tester, (5866 series) at 0.21 mm/s. The initial materials were characterized prior to compaction and consolidation.

The primary phase (Al) has a nominal size of 100 μm with a size range (particle distribution) from the submicron to ~ 175 , a nominal density of 2.699 g/cm^3 @ RT and EDX confirmed it was Al-1100 aluminum (Figure 6c). The powder morphology consisted of rounded and irregular granules with microdendritic structures, resulting from the vendors' powder processing, as shown in the SEM images in Figures 6a and b. Figure 7a shows a TEM image of the MWCNT aggregate mixture measuring 30 to 40 nm. The shapes were a mixture of fullerenes and naturally short MWCNTs (SLA Tubes). EDS results found the powder to be mainly carbon (Figure 7b).

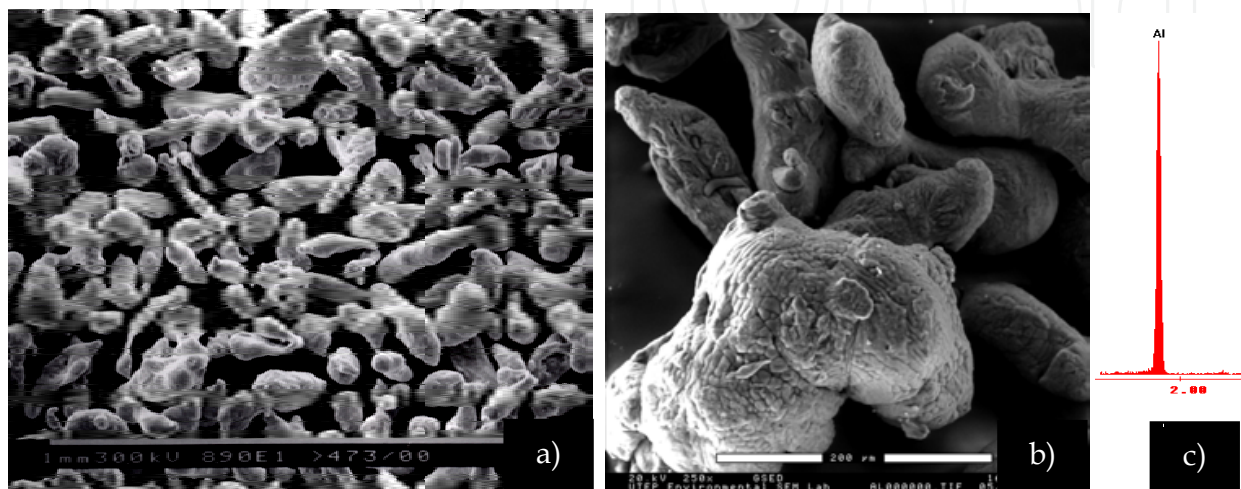


Fig. 6. Aluminum powder, with a nominal size of 150 mesh, at a) low (light microscopy) and b) high magnification (SEM) micrographs and c) EDS spectrum.

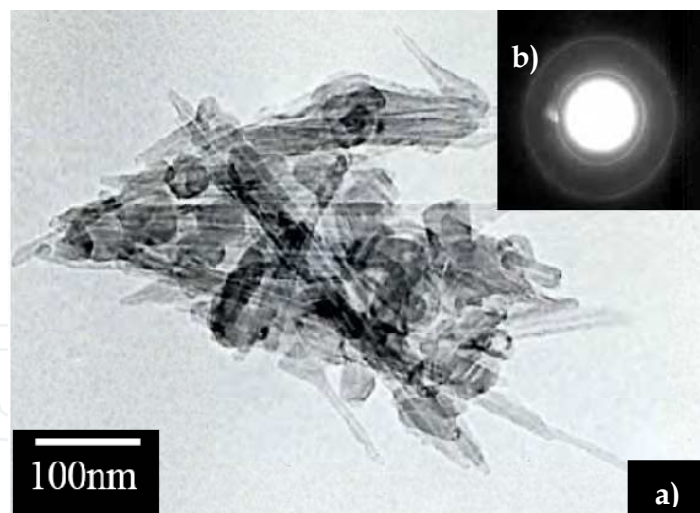


Fig. 7. Original starting material of MWCNT aggregate mixture.

Images in Figure 8 illustrate that the starting Al particles had a micro-dendritic microstructure (Figure 8a) resulting from the powder processing. Figure 8b shows for comparison a light micrograph of a section view where the micro-dendritic structure is observed to be preserved both for the shock wave consolidated (SWC) aluminum monolith and for the consolidated Al/5%MWCNT system (Figure 9b). Figure 8b also shows the high degree of compaction achieved in the aluminum single-phase during consolidation as

evidenced by the absence of voids in the microstructure especially at triple grain points. This is confirmed by the achieved density of $\sim 98\%$ (by Archimedean method), which is consistent with a SWC process

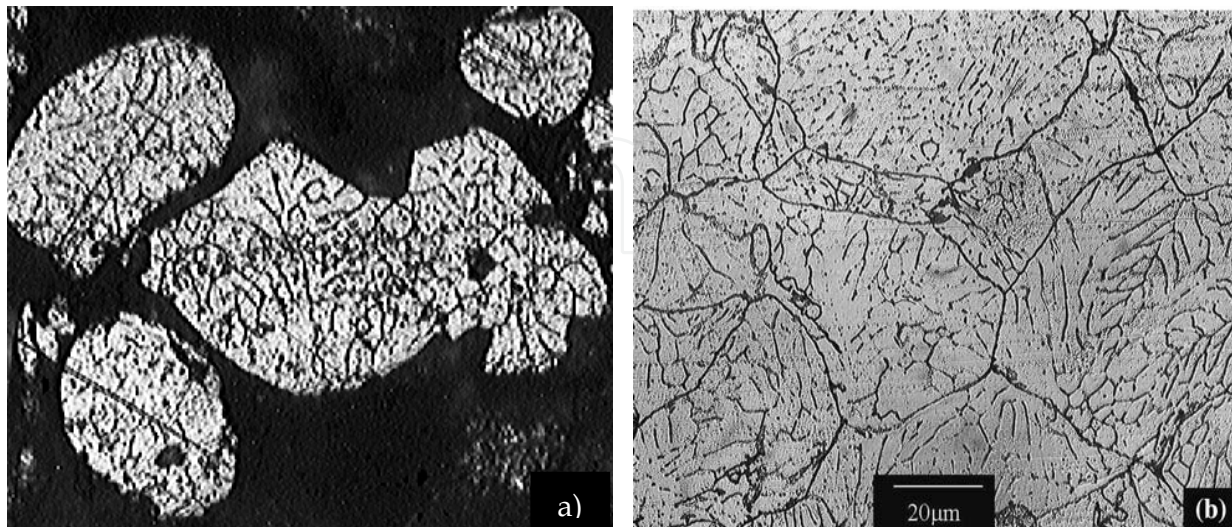


Fig. 8. (a) Light microscope image of Al-powder microstructure showing microdendritic structure and (b) light microscope image of consolidated Al phase.

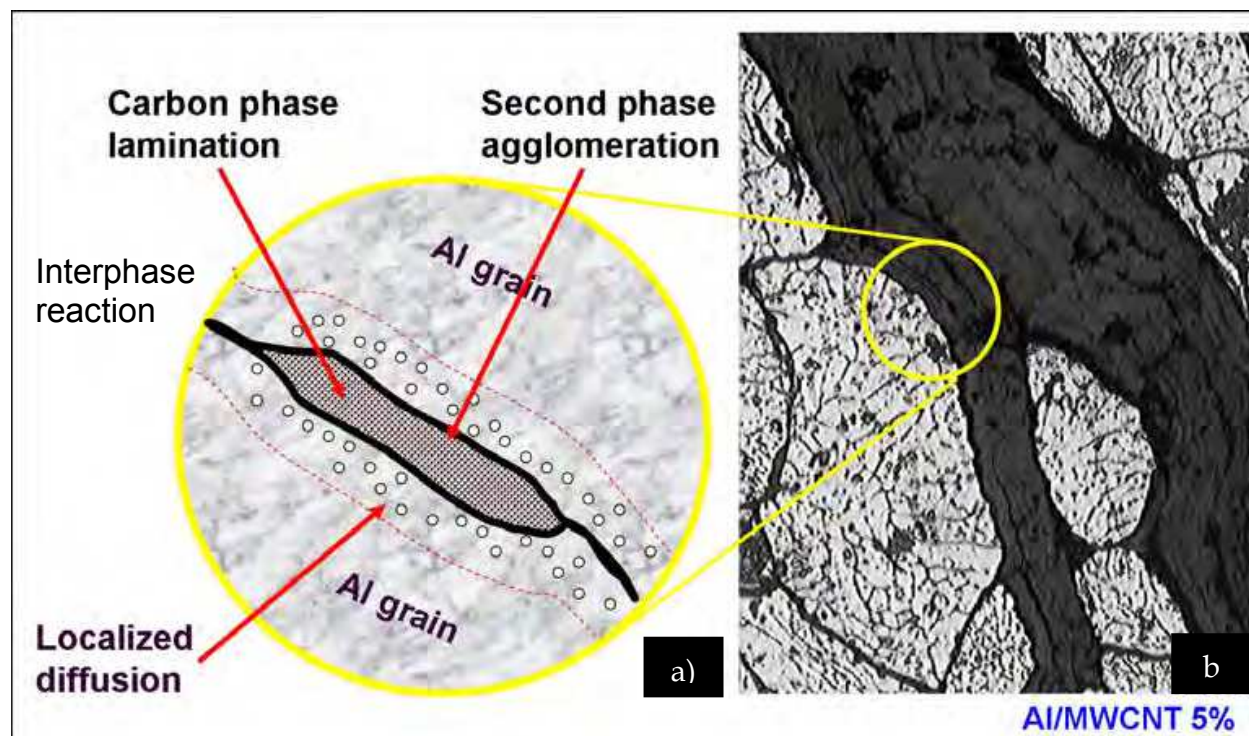


Fig. 9. a) Representation of different interactions between phases occurring during the fabrication of a metal/CNT systems and b) an image of an Al/5%MWCNT sample.

3.1 Hardness measurements

Characteristics of optimum explosive compaction strengthening include a marked increase in hardness that is mostly uniform over the cross section of the consolidated materials. As described later, the formation of agglomerates along with their distribution in the continuous phase and their size difference as compared to the continuous phase aluminum grains is expected to result in hardness variations between the consolidated systems. However the increase in hardness is mainly associated with the SWC of the aluminum continuous phase. In contrast to the initial Al powder Vickers hardness of HV 24 (HRE 22, by conversion), the explosively consolidated aluminum samples exhibit a hardness of HV 43 (HRE 40), which represents a 79% increase in hardness. The average hardness contribution from the two-phase regions (characteristic of Rockwell E scale) exhibits the ability of aluminum to shock-harden as illustrated in the TEM images of Figure 10, where it is shown the shock-induced dislocation substructures along with dynamically recrystallized regimes. There was a decrease in hardness associated with SWC of the two-phase systems as compared to the SWC of the aluminum. The Al/2%MWCNT sample had a hardness decrease to HRE 39. Increasing the volume fraction of CNT aggregates further to Al/5%MWCNT significantly lowered the hardness reading to HRE 33. This represents a decrease of ~18% from the consolidated aluminum (HRE 40). This trend in hardness reduction is consistent with Feng et al (2005), who concluded that the agglomeration of carbon nanotubes at an increasing volume fraction leads to a decrease in hardness and will eventually lead to failure under an applied load (decrease in yield strength). Feng et al (2005) also describes two weaknesses that can be found in an Al/MWCNT system: weak bonding of the agglomerate to the Al phase and also a weak bonding between the nanotube materials. It is this weak bonding that causes such a decrease in hardness. Consolidated aluminum samples showed a 0.2% offset yield for the Al of 120 MPa with a UTS of 140 MPa and an elongation of 6.6%. When comparing this data to the nominal Al-1100 data (for 1.6 mm samples) (ASM Handbook, 1990) there is an increase of ~28% in strength and a 45% reduction in the Al-base plasticity (from 110 MPa and 12% respectively). The Al/2%MWCNT aggregate TPS failed at an elongation of ~2% which is somewhat commensurate with results for two-phase Al-A356/20% fly ash (volume) where elongation was observed to be between 1 and 2% (Withers, 2005).

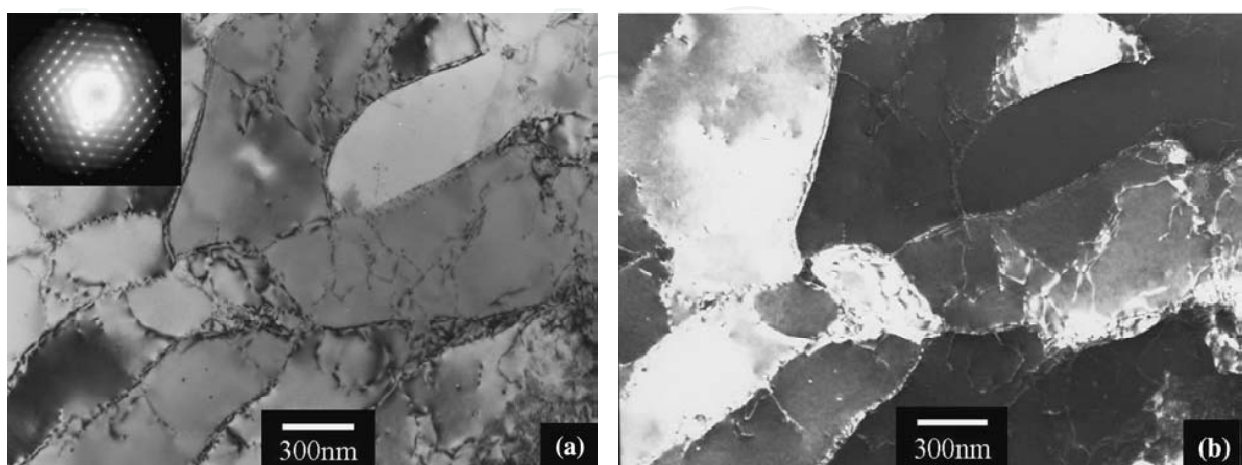


Fig. 10. (a) Bright-field and (b) dark-field TEM images showing shock-induced dislocation substructures along with dynamically recrystallized regimes.

4. CNT second phase behaviour

In addition to the achieved mechanical properties, images of the obtained samples can illustrate a set of resultant possibilities on the distribution of the second phase (refer to Figure 9a) achieved in a consolidated metal/CNT and, more specific in our case, Al/CNTs systems. As described by Salas et al (2007) the second phase can consolidate in micron-sized agglomerates (reported by Lijie et al, 2006; Laha et al, 2009; and Lim et al, 2009) and also as CNTs arranged in lamellae agglomerates (as later reported by Lim et al, 2009) or entangled clusters (Laha et al, 2009; and Lim et al, 2009). The Al-CNTs interphase can be dispersed in a connected or disrupted network (also reported by Kim et al, 2006), can have a non-reacted localized diffusion at the Al grain surface (as recently reported by Laha et al, 2009) and/or can react totally/partially at the Al-Al grain boundary forming Al_4C_3 (Lijie et al, 2006; and Alba-Baena et al, 2008).

4.1 Micron-sized agglomerates

A simplified model for the microstructure of a TPS consists of two parts, i.e. an Al/agglomerated MWCNT aggregate region and an aggregate mixture free or continuous phase region. CNTs tend to agglomerate at the primary-phase grain boundaries as illustrated in Figure 11. Figure 11a also shows large agglomerates characteristic of a high volume fraction (Al/5%MWCNT) two-phase system. The microstructure shown in Figure 11 demonstrates the high degree of compaction achieved in the aluminum phase. This is consistent with SWC process as evidenced by the absence of voids in the microstructure, especially at triple grain points. Images in Figure 11a and b reveal agglomerates located mainly at the aluminum grain boundaries and are not homogeneously distributed in the Al continuous phase but rather the carbon nanotube material is densely distributed in localized regions along the continuous phase. Figure 11b shows a higher magnification view of the agglomerations of MWCNT aggregate particles and the pore-free surface of the Al phase. Along with those observations for the aluminum monolith, i.e. low porosity and high densification, the SWC effect and plastic flow results in the accommodation of the agglomerated MWCNT aggregate mixture into the aluminum-phase grain that preserves its structure intact (shown previously by Figure 8b).

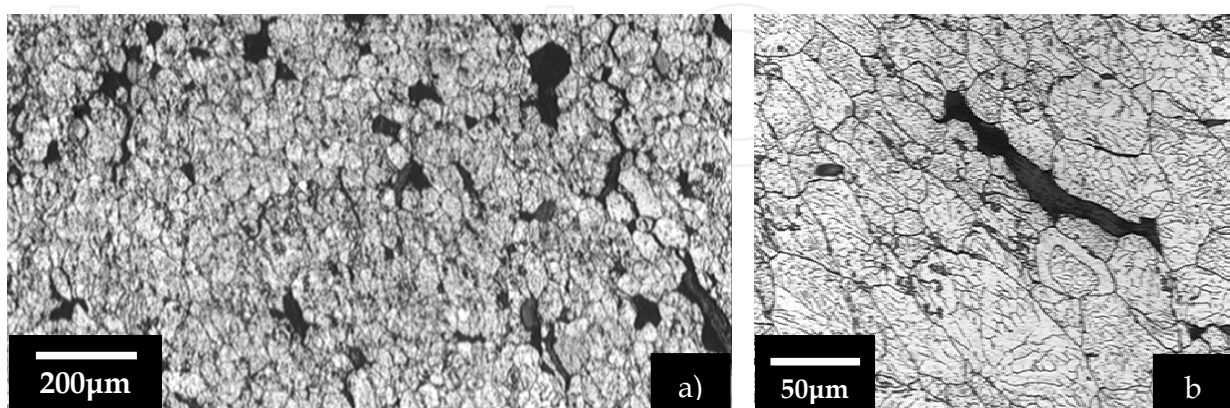


Fig. 11. a) Microstructure of an Al/5%MWCNT sample showing the high degree of compaction achieved and b) a magnified view showing the intact aluminum-grain interior but plastically deformed to accommodate the MWCNT aggregates.

4.2 Lamellae structures

CNT phase agglomerations can exhibit two types of structures: entangled clusters (described later) and laminar type arrangements (lamellae structures). This interesting laminar feature is shown in Figure 12 where the SEM view (Figure 12a) of a polished surface section (of an Al/2%MWCNT system) exhibits the laminated flow marked by the gaps separating the consolidated regions. The bonding between the MWCNT aggregate phase and the Al appears to be optimum at the arrow.

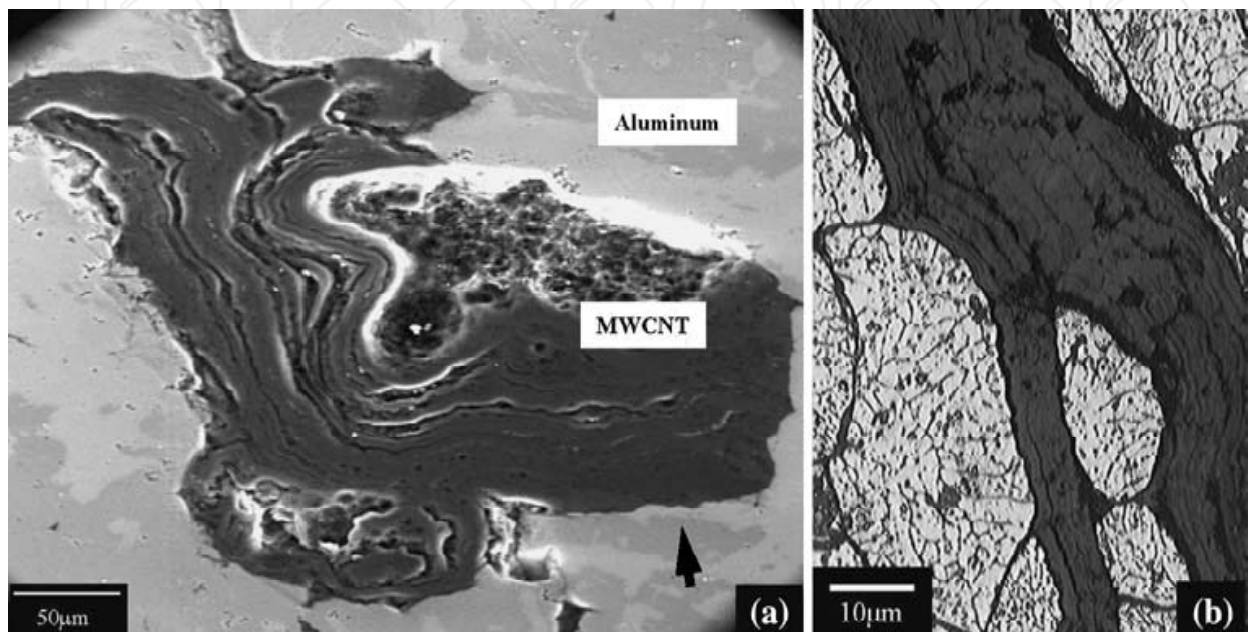


Fig. 12. a) SEM image showing a lamellae structure of a MWCNT agglomeration with bonding between phases (as indicated by arrow) and b) Light microscopy detail of the carbonaceous-laminated feature.

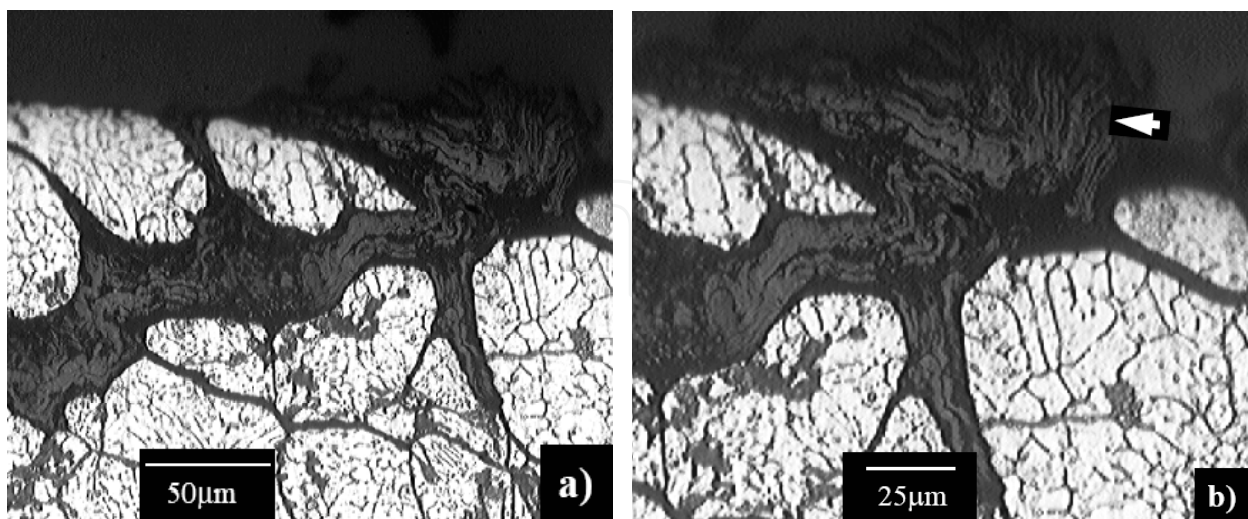


Fig. 13. a) Light microscopy image of the delaminating features observed in the carbonaceous phase on a sample edge b) arrow shows detail of the delaminating feature.

The apparent fully consolidated laminar structure, shown in Figure 12b, is resultant of the compression of such layers by the SWC process or by other highly energetic processes such as friction stir processing (Lim et al, 2009). These carbonaceous-layer regions have been reported in recent literature but not characterized. However, it is believed that such laminated regions are comprised of multi concentric tubes and fullerenes and are compacted together by the SWC process along the basal planes which experience weak Van der Waals forces. It is the attribution of these weak Van der Waals forces between layers (Figure 13) that can be a starting point to the the decohesion and delamination shown by the arrow in Figure 13b. Such delaminating features observed in the carbonaceous phase and shown in Figure 13 have similar characteristics to that observed by Peikrishvili et al (2001) during the explosive compaction of Ni and graphite powders.

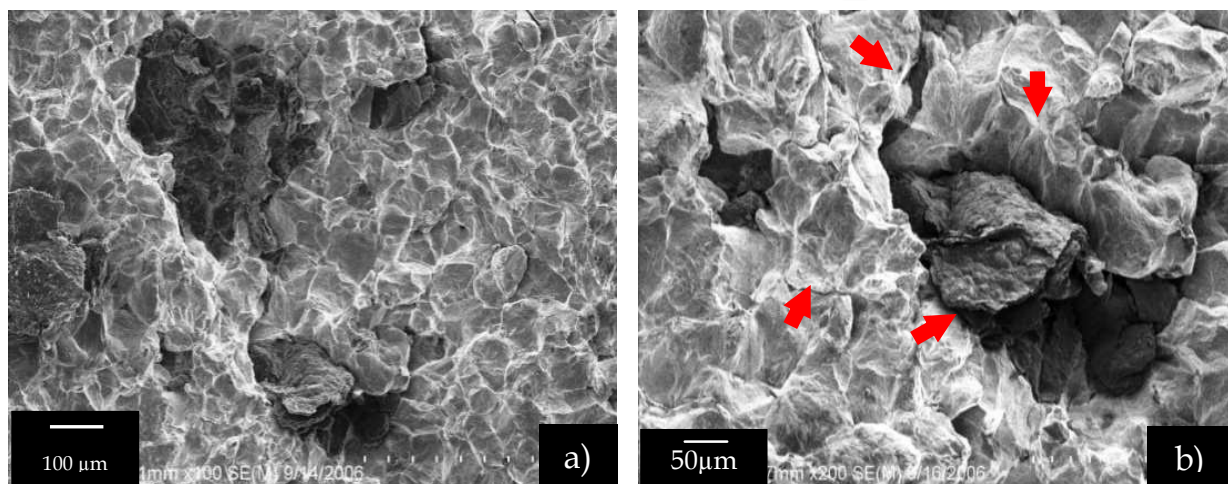


Fig. 14. a) The ductile-dimple fracture marked by intergranular failure between aluminum grains and micron-sized agglomerates of second phase and b) fracture surface that demonstrate some of the fracture modes exhibited by this TPS.

Figure 14 shows the second phase (aggregate) accommodation along the grain boundaries of the continuous aluminum phase which is observed and expected in a SWC two phase system. As known, the aggregates size variation can be the result of the mixing process and the tendency of the MWCNTs and multi-concentric fullerenes to agglomerate. Figure 14a also shows the ductile-dimple fracture characteristic of the aluminum continuous phase as noted by the intergranular failure between aluminum grains and micron-sized lamellae agglomerates that have been pulled apart (noted in Figure 14b). Figure 14b is an SEM image of a fracture surface that demonstrates some of the fracture modes exhibited by this TPS. The arrow at the top indicates the ductile behavior characteristic of the aluminum continuous phase. Intergranular particle cracking can be observed between aluminum grains in the continuous phase shown by the arrow to the left in the image. This intergranular particle failure is also exhibited between the aluminum grains and the agglomerated second phase as indicated by the arrow at the bottom of the Figure. A transgranular fracture mode is demonstrated by the region marked by the arrow to the right in the image. Here the agglomerate particle pulled apart from itself in a delayering or decohesion fashion and is pointed out by the arrow at the center of the image. Figure 15a is further detail of the layering agglomerate where the delayering mechanism after fracture has been previously described in Figure 13.

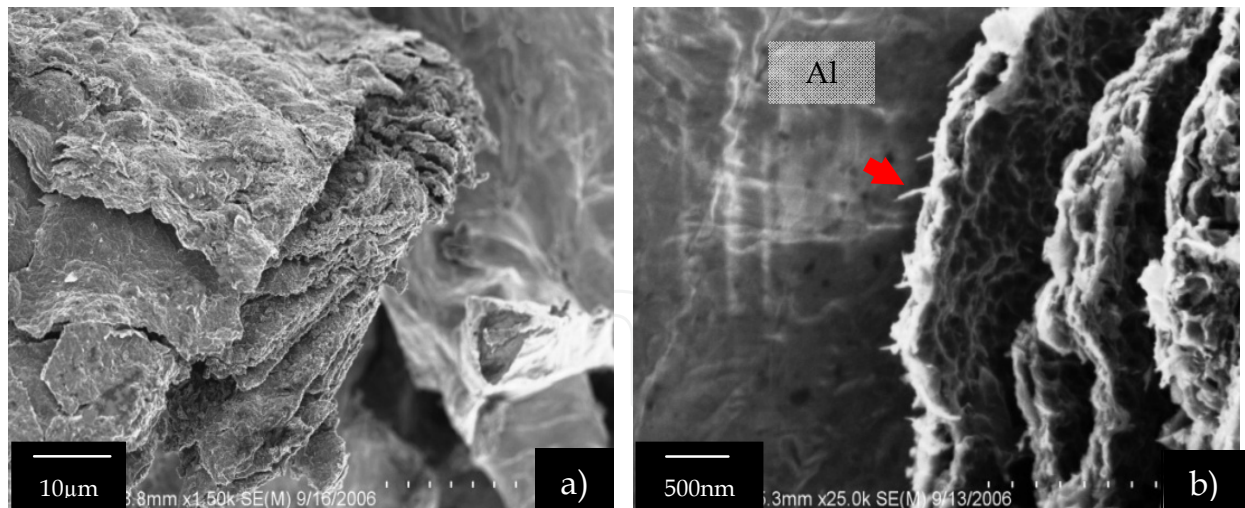


Fig. 15. a) Detail of the layering agglomerate and b) MWCNTs pulling out of the aluminum phase leaving characteristic holes.

The laminar appearance of the consolidated graphitic phase suggests that of pyrolytic graphite, especially in Figure 15b which shows details of the laminar structure and delamination of the carbonaceous arrangement. Also the Al-C interphase interaction is observed (arrow, Figure 15b) where the MWCNTs are seen emanating from the C-phase surface and MWCNTs are pulled out of the aluminum phase material and leaving characteristic holes in the surface. Finally, Figure 16 exemplifies the Al/laminar-agglomerate debonding showing a top layer of thin layered agglomerate lying on top of grain boundaries and exhibiting ductile dimple features (arrow) on the carbonaceous material which corresponds to that observed in Figure 15b.

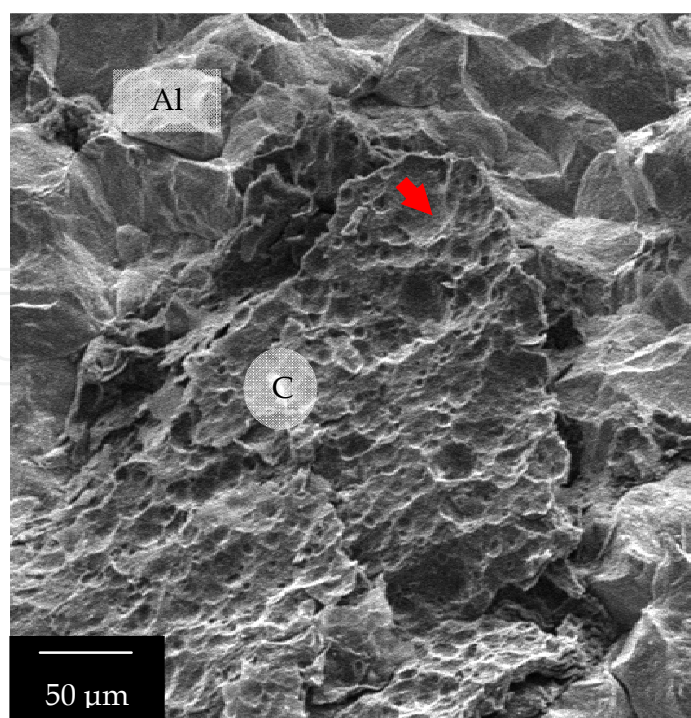


Fig. 16. Example of dimple features (arrow) of the carbonaceous material.

4.3 Entangled clusters

The agglomerate shown in Figure 17a reveals more on the nature of the entangled clustering behavior observed in between the laminar arrangements and smaller agglomerated regions. Here CNTs debond easily from the carbonaceous material. Figure 4.17b shows an enlarged view of this entangled carbonaceous material disaggregating from the Al surface (arrow). This also illustrates poor Al-C bonding that may be responsible for the reduction in elongation of this TPS's tensile samples along with the poor tensile strength.

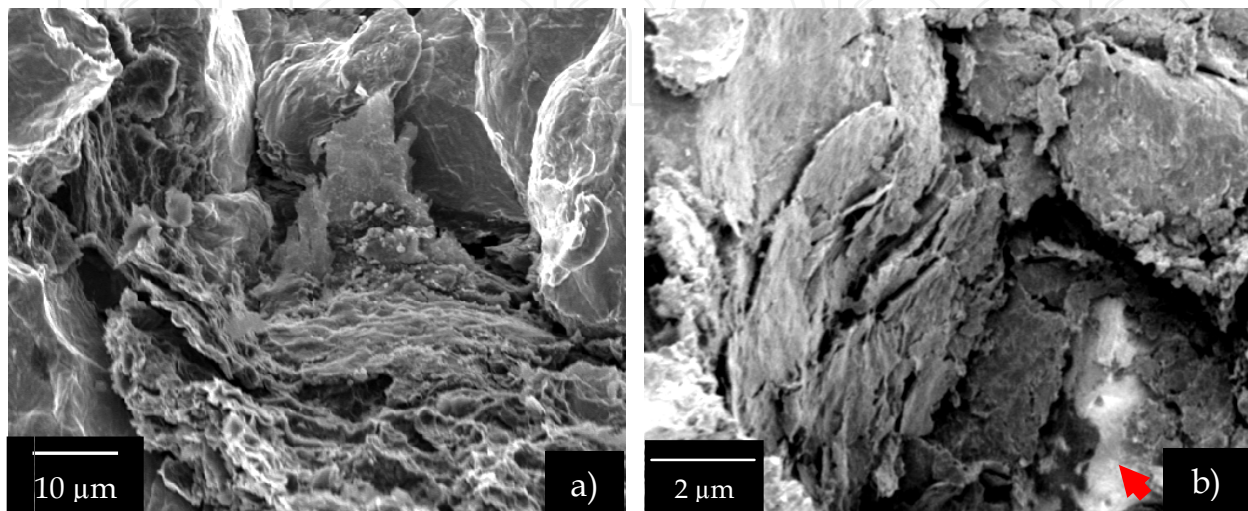


Fig. 17. a) Entangled carbon cluster surrounded by ductile-dimple fractured Al grains and b) detail view of a cluster sitting at an Al grain surface.

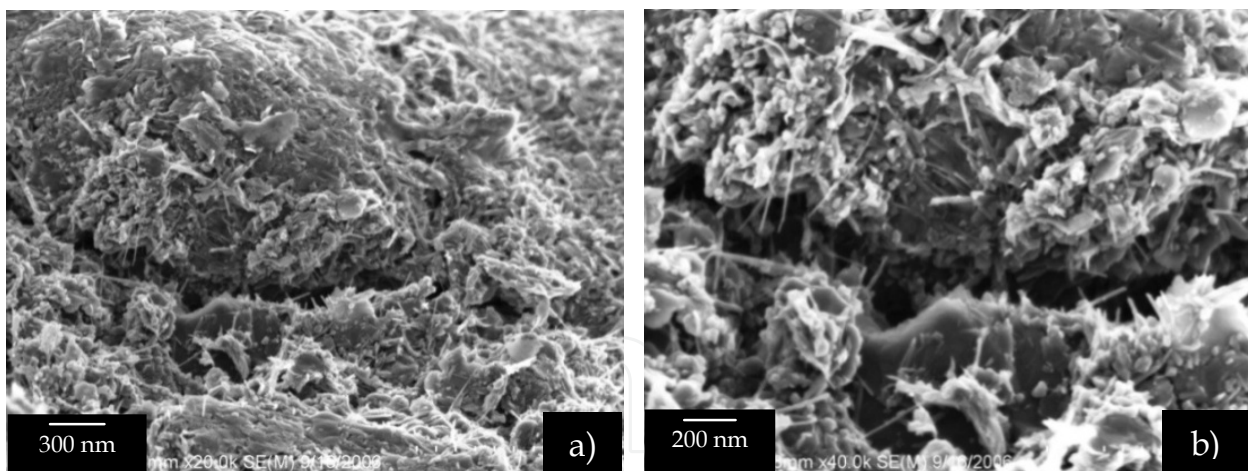


Fig. 18. a) Entangled and partially consolidated carbon phase cluster. b) Detailed view showing undamaged and randomly dispersed carbon nanotubes along the fractured surface.

An entangled cluster characterization is shown in the sequence of images shown by Figures 17-19. Figure 18a is a closer look at an entangled cluster showing different carbon phases and unconsolidated carbon nanotubes lying in between the continuous metal phase. Figure 18b is a detailed view of the cluster where the partially consolidated carbon phase is clustering carbon nanotubes with other carbonaceous phases from the original material and is a result of the SWC process. As the magnification is increased in Figure 19a the fractured

graphitic phase begins to resemble features of the original MWCNT aggregate material shown in Figure 7b. The MWCNTs and individual, multiconcentric fullerenic particles and graphitic particles are clearly visible in Figure 19b as characteristic of these Al/agglomerated MWCNT aggregate clusters.

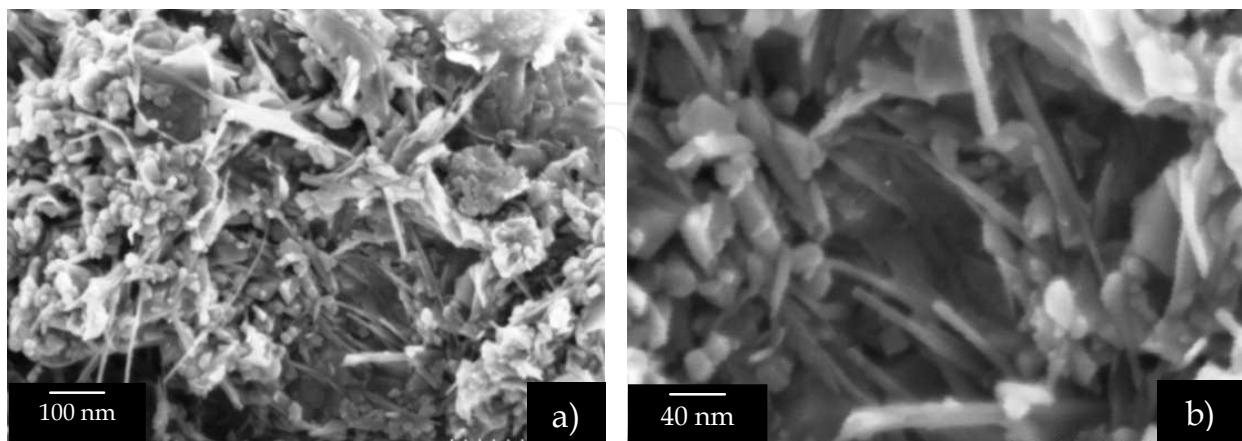


Fig. 19. Sequence showing the consolidated carbonaceous clusters along with entangled MWCNTs.

4.4 Interface diffusion

Smaller agglomerations (Figure 20) can be found in the Al-Al interphase of the TPS. These CNT agglomerations are shown as flaky unconsolidated carbonaceous particle material. Also observed are individual CNTs distributed along the Al grains interface. An interesting observation is shown in the magnified view of Figures 20a and b which are of an aluminum grain boundary that has experienced intergranular fracture. At the crevice separating these two aluminum grains we can see individual CNTs protruding out (see arrow), also there is no evidence that the nanotube had been embedded into the continuous phase as described for the inter-type of TPSs (shown previously in Figure 1).

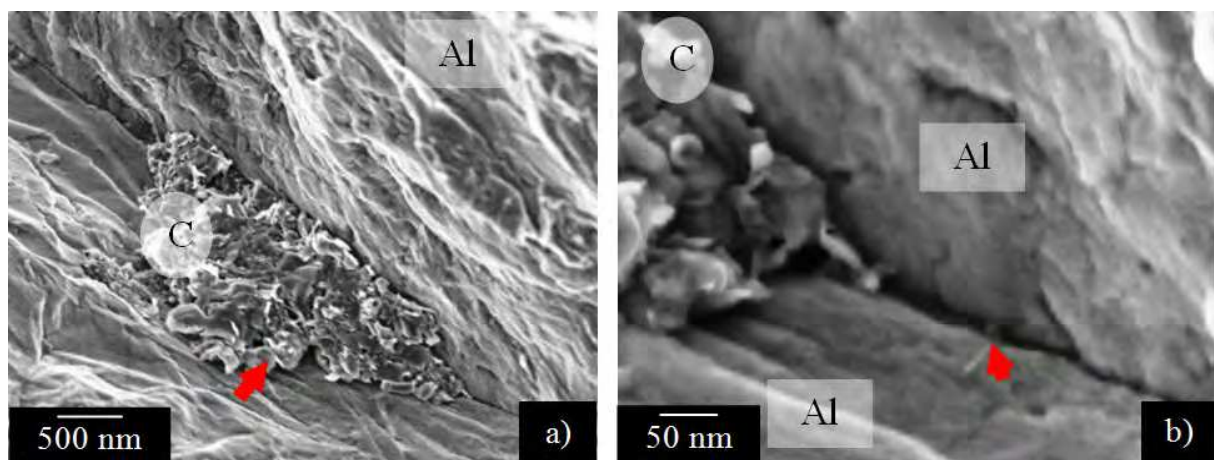


Fig. 20. A sequence showing a cluster of carbonaceous material at the Al-Al interface.

4.5 Localized diffusion

Figure 21a is a TEM micrograph for the consolidated Al/5%MWCNT TPS which shows (marked by the right arrow) that there appears to be evidence of MWCNTs embedded into the aluminum continuous phase. This embedment indicates good intra-facial bonding between the two phases that is beneficial for load transfer. These observations spur further investigation to the nature of the bonding between the MWCNTs and the aluminum continuous phase because it is an indication that there is a retention of CNTs in the continuous phase. Also in this TEM photo, aggregate material appears to lie in between the grain boundaries (left arrow) as evidence of the intergranular bonding of CNTs. This bonding also enhances the load transfer between phases and grains (refer to Figure 2). These features are also observed in Figure 21b which clearly shows remnants of etched Al grains (arrow) intermixed with the MWCNT aggregate material which is representative of a two-phase system and the agglomeration of the second phase. The edge of the thin area to the right in Figure 21b exhibits some apparent carbon/fullerene nanoparticle consolidation, but the nature of this consolidation is unclear. The SAED pattern insert is also consistent with overlapping, etched Al grains or particles and carbonaceous material.

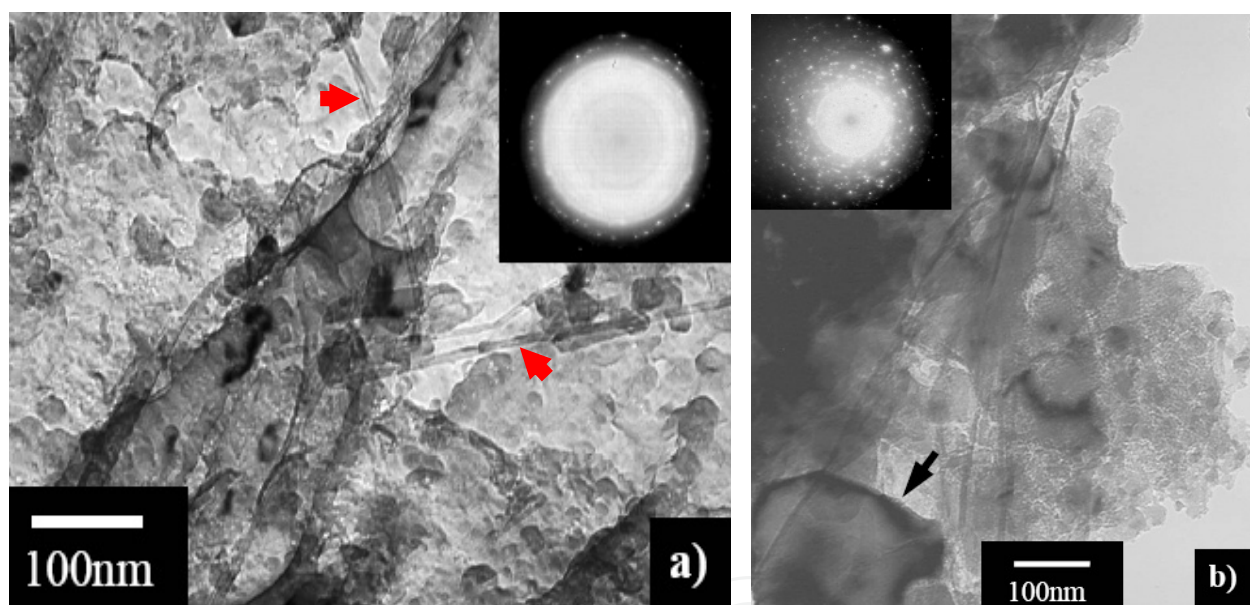


Fig. 21. TEM images of the 5%MWCNT aggregate TPS showing the CNT diffusion in and between the Al grains.

Images in Figures 22 and 23 are of a microscopic view which shows another detail in the aluminum continuous phase surface. After the SWC, the carbon diffusion at the interface is shown as having experienced partial consolidation and being accompanied by agglomerations of the carbon phase. Figure 22 illustrates the localized dispersion of CNTs along the continuous phase resultant from the SWC process; a $\sim 1.5 \mu\text{m}$ agglomeration at the Al grain surface did not consolidate in the described laminar structure but dispersed and the CNTs that pulled out from the aluminum phase surface are shown (arrows). The fractured sample in Figure 23 illustrates how the reduction of the agglomeration sizes (below $10 \mu\text{m}$ in diameter) may improve the two-phase system's mechanical response while preserving the carbonaceous phase properties. With the use of smaller second-phase volume fractions and the reduction of the agglomeration sizes (or its elimination), improvements in the dispersion

of the MWCNT phase are expected. The experimentation of these changes in the improvements in the consolidation of a TPS may lead to the consolidation of MMCs characterized by the matrix grain-size control and the MWCNT will promote the primary phase and /or TPS mechanical responses.

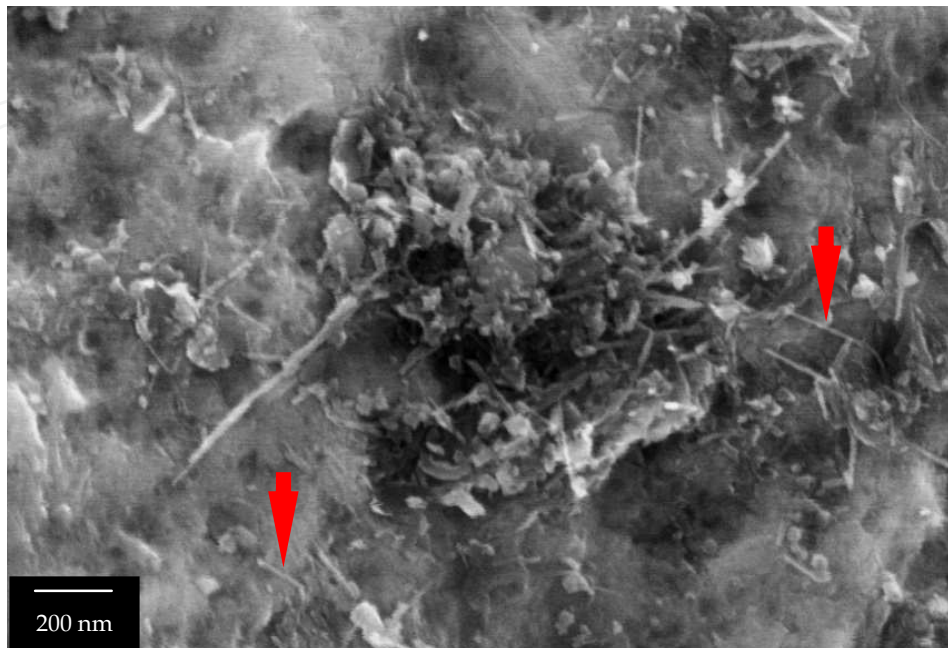


Fig. 22. Magnified image of the carbon nanotubes which can be seen to lie undamaged between grains.

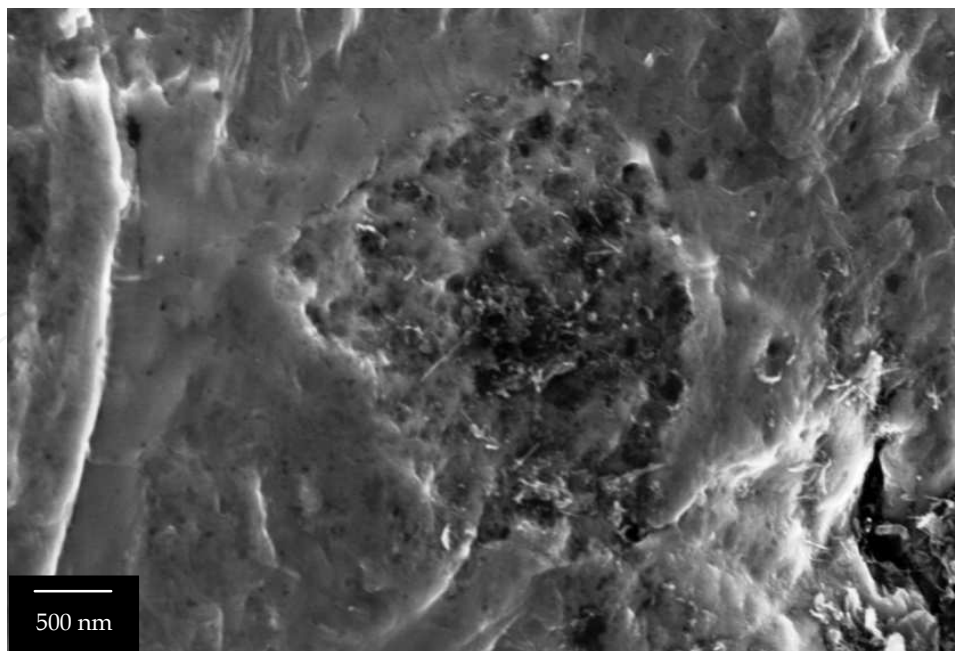


Fig. 23. An agglomerate appears to have fallen out of the continuous phase due to the inconsistency of the aggregate bonding.

4.6 Al-C consolidation

Figure 24 exemplifies the consolidation of the Al-C TPS exhibiting good bonding between the aluminum continuous phase and the second phase aggregate mixture. The carbonaceous material, indicated by the arrow on the left, has bonded to the ductile-continuous-aluminum phase. This image also shows several areas of strong bonding marked by arrows. The arrows on the right illustrates an area where the bond strength is strong enough that here failure has occurred as a result of ductile failure indicated by regions above and below the bonded carbon phase material.

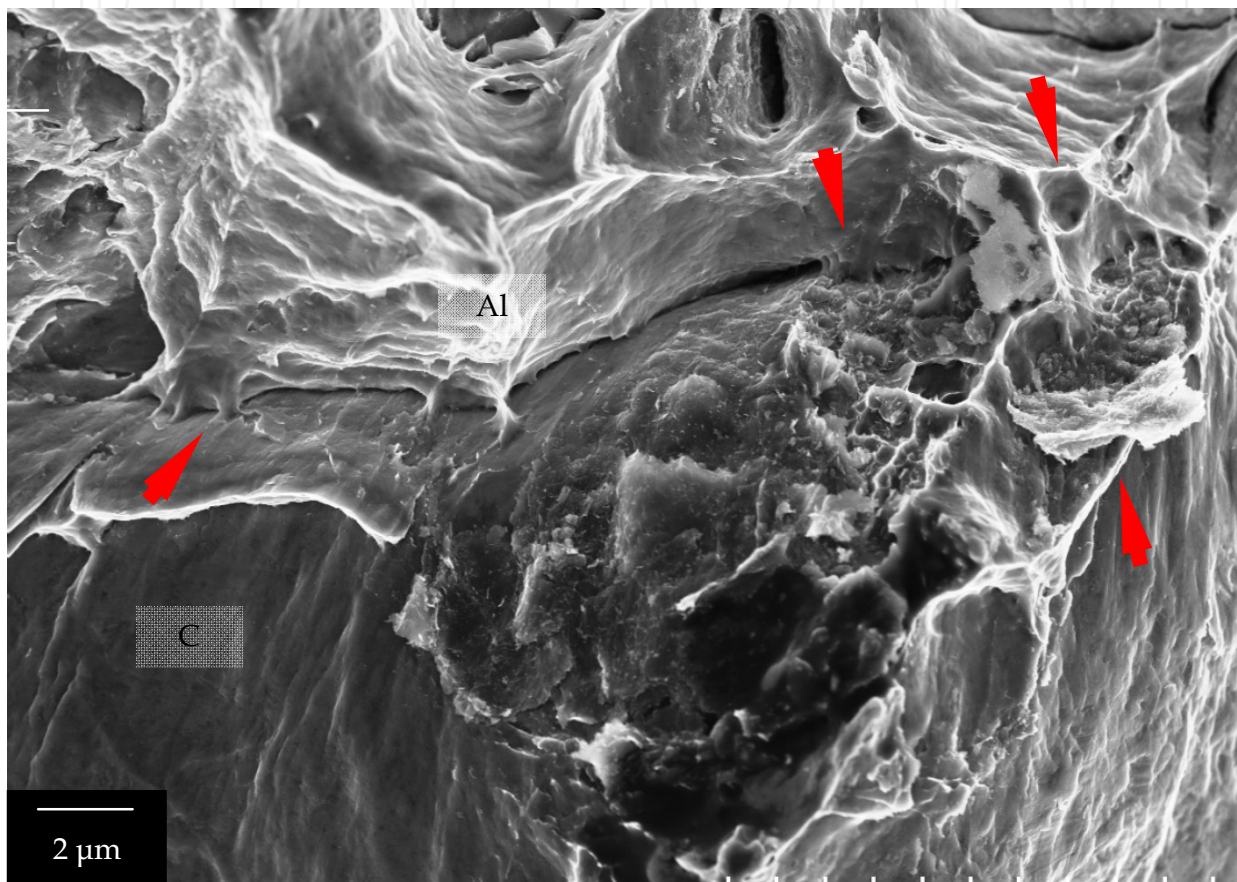


Fig. 24. Further evidence of the degree of bonding between the continuous phase and the second phase showing several areas of strong bonding marked with arrows.

4.7 Al-C Reaction

During observations on Al/MWCNT systems there was no Al-C reaction, but this can occur due to the Al plastic flow and CNT reactions through the SWC; as previously described by Alba-Baena et al (2008) for Al-SiC systems. They report nanoreaction results as hexagonal platelet-shapes (Al_3C_4) and spherical Si particles distributed at the aluminum surface. Figure 25 illustrates the observed chemical reaction products from an Al/21%SiCnp system forming a layer at the aluminum phase surface and a detail view of the Al_3C_4 platelets formed after SWC process, but the details of these reactions are still unknown.

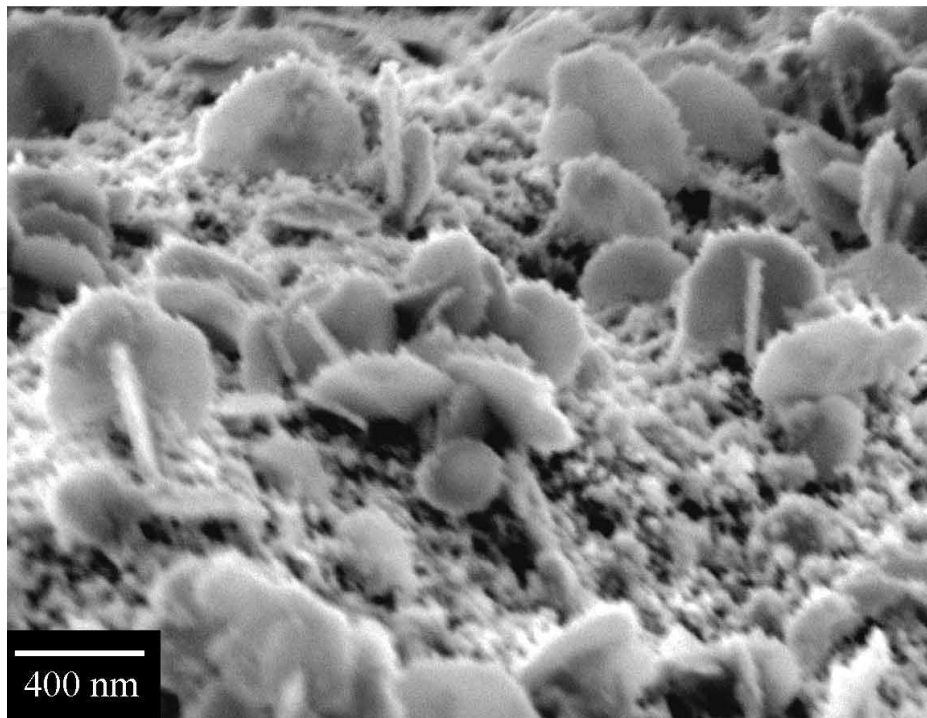


Fig. 25. Image of Al₃C₄ platelets at Al grain surface in an Al/SiC TPS (from Alba-Baena et al, 2008).

5. Conclusion

The ability in incorporating carbon nanotubes to structural and functional TPS will lead to the improvement and tailoring in the strength-to-weight ratios on materials for a wide variety of industries. This chapter has outlined further micro-nanosystems knowledge about preparing materials and using SWC for future developments. Al-MWCNT aggregate two-phase composites of 2 and 5% volume fraction were fabricated using a single tube shockwave consolidation process. This reports evidence on the achievement of aluminum-based two-phase systems describing different Al/CNTs interactions. Particularly notable is where CNT agglomerates of these two-phase systems have been shock consolidated into a contiguous phase region, and this regime can be bonded, monolithically, to the consolidated aluminum particle regime. The carbonaceous, MWCNT aggregate phase can exhibit a shock-induced, laminated flow-type, consolidation feature that appears to spread throughout the primary phase (Al) grain boundaries and consolidates as large phase regions at the aluminum triple points. At a fractured sample the MWCNT aggregate phase shown the entangled agglomerates and surface dispersion along Al grains, observed when MWCNTs pull out of the aluminum phase at fracture as well. Present descriptions and observations are in agreement with other studies that have determined that the reinforcement efficiency on the mechanical properties is dependent on dispersion, volume fraction and interfacial strength.

6. References

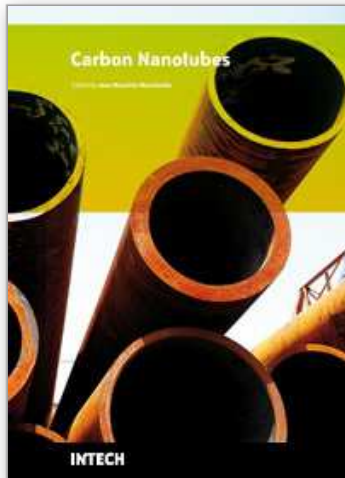
- Ajayan, P. M.; Schadler, L. S. and Braun P. V. (2004). *Nanocomposite Science and Technology*, Wiley & sons, ISBN: 3-527-30359-6.
- Akbulut, H.; Durman, M. and Yilmaz, F. (1998). *Dry wear and friction properties of δ -Al₂O₃ short fiber reinforced Al-Si (LM 13) alloy metal matrix composites*, *Wear*, vol. 215, No. 1-2, pp.170-179, ISSN: 0043-1648.
- Alba-Baena, N. G.; Salas, W. and Murr, L. E. (2008). *Characterization of micro and nano two-phase regimes created by explosive shock-wave consolidation of powder mixtures*, *Materials Characterization*, vol. 59, pp. 1152-1160, ISSN: 1044-5803.
- ASM Handbook, (1990). *Properties and selection: Nonferrous alloys and special purpose materials*, ASM International, pp. 3-215, ISBN 10: 0-87170-378-5.
- Bakshi, S. R.; Singh, V.; Balani, K.; McCartney D. G.; Seal, S. and Agarwal, A. (2008). *Carbon nanotube reinforced aluminum composite coating via cold spraying*, *Surface & Coatings Technology*, vol. 202, pp. 5162-5169, ISSN: 0257-8972.
- Cha, S. I.; Kim, K. T.; Arshad, S. N.; Mo, C. B. and Hong, S. H. (2005). *Extraordinary Strengthening Effect of Carbon Nanotubes in Metal-Matrix Nanocomposites Processed by Molecular-Level Mixing*, *Advanced Materials*, vol. 17, 11, pp. 1377-1381, ISSN: 0935-9648.
- Chen, W.; Tu, J.; Wang, L.; Gan, H.; Xu, Z.; and Zhang X. (2003). *Tribological application of carbon nanotubes in a metal-based composite coating and composites*, *Carbon* 41, pp. 215-222, ISSN: 0008-6223.
- Chen, X. Xia, J. Peng, J. Li, W.; Xie, S. (2000). *Carbon-nanotube metal-matrix composites prepared by electroless plating*, *Composites Science and Technology*, vol. 60, 2, pp. 301-306, ISSN: 0266-3538.
- Chen, T.; Hampikian, J. M.; and Thadhani, N. N. (1999). *Synthesis and characterization of mechanically alloyed and shock-consolidated nanocrystalline NiAl intermetallic*, *Acta materialia*, vol. 47, 8, pp. 2567-2579, ISSN: 1359-6454.
- Collins, Ch.; Thadhani, N. N.; and Iqbal, Z. (2001). *Shock-compression of C-N precursors for possible synthesis of β -C₃N₄*, *Carbon*, vol. 39, pp. 1175-1181, ISSN: 0008-6223.
- Counihan, P. J.; Crawford, A. and Thadhani N. N. (1999). *Influence of dynamic densification on nanostructure formation in Ti₅Si₃ intermetallic alloy and its bulk properties*, *Materials Science and Engineering A*, vol. 267, pp. 26-35, ISSN: 0921-5093.
- Csanady, A.; Sajo, I.; Labar, J. L.; Szalay, A.; Papp, K.; Balaton, G. and Kalman, E. (2006). *Al-Pb nanocomposites made by mechanical alloying and consolidation*, *Current Applied Physics*, vol. 6, pp. 131-134, ISSN: 1567-1739.
- Deribas, A. A.; Simonov, P. A.; Filimonenko, V. N. and Shtertser A. A. (2001). *Chap. 42: Bulk samples of intermetallics, obtained by shock compaction*, *Fundamental Issues and Applications of Shock-Wave and High-Strain Rate Phenomena*, K.P. Staudhammer, L.E. Murr, and M. A. Meyers, (Eds.), Elsevier Science Ltd., Amsterdam, pp. 331-336, ISBN: 008043896-2.
- Dresselhaus, M. S.; Dresselhaus G. and Avouris P. (2008). *Carbon nanotubes: synthesis, structure, properties and applications*, Springer, ISBN: 978-3-540-72864-1.
- Drost, H.; Friedrich, M.; Mohr, R. and Gey, E. (1997). *Nanoscaled Si-C-N-composite powders with different structures by shock-wave pyrolysis of organic precursors*, *Nuclear Instruments and Methods in Physics Research B*, vol. 112, pp. 598-601, ISSN: 0168-583X.

- Epanchintsev, O. G.; Zubchenko, A. S.; Korneyev, A. E. and Simonov, V. A. (1997). *Highly-efficient shock-wave diamond synthesis from fullerenes*, Journal of physics and chemistry of solids, vol. 58, 11, pp. 1785-1788, ISSN: 0022-3697.
- Everett, R. K. and Arsenault, R. J. (1991). *Metal Matrix composites: processing and interfaces*, Academic press LTD, Elsevier Science & Technology Books, ISBN: 012341832-1.
- Feng, Y.; Long Yuan, H.; Zhang, M. (2005). *Fabrication and properties of silver-matrix composites reinforced by carbon nanotubes*, Materials Characterization, vol. 55, pp. 211-218, ISSN: 1044-5803.
- Glade, S. C. and Thadani, N. N. (1995). *Shock consolidation of mechanically alloyed amorphous Ti-Si powders*, Metallurgical and Material Transactions A, vol. 261, p. 2565, ISSN: 1073-5623.
- Jin, Z. Q.; Chen, K. H.; Li, J.; Zeng, H.; Cheng, S. F.; Liu, J. P.; Wang, Z. L. and Thadhani, N. N. (2004). *Shock compression response of magnetic nanocomposite powders*, Acta Materialia, vol. 52, pp. 2147-2154, ISSN: 1359-6454.
- Jordan, J. L. and Thadhani, N. N. (2001). *Chap. 39: Synthesis of Ti-based metal-like ternary ceramic compounds by dynamic densification and reaction synthesis* in Fundamental Issues and Applications of Shock-Wave and High-Strain Rate Phenomena, K. P. Staudhammer, L. E. Murr, and M. A. Meyers, (Eds.), Elsevier Science Ltd., Amsterdam, pp. 305-312, ISBN: 008043896-2.
- Kawaka, A.; Soma, T. and Saito, S. (1974). *Structure determination of boron nitride transformed by shock compression*. Japanese Journal of Applied Physics, vol. 13, 5, p. 891, ISSN: 0021-4922.
- Kennedy, G.; Keller, A.; Russell, R.; Ferranti, L.; Zhai, J.; Zhuo, M. and Thadhani, N. N. (2001). *Chap. 9: Dynamic mechanical properties of microstructurally-biased two-phase $TiB_2+Al_2O_3$ ceramics* in Fundamental Issues and Applications of Shock-Wave and High-Strain Rate Phenomena, K. P. Staudhammer, L. E. Murr, and M. A. Meyers, (Eds.), Elsevier Science Ltd., Amsterdam, pp. 63-70, ISBN: 008043896-2.
- Kimura, Y. (1963). *Formation of zinc ferrite by explosive compression*, Japanese Journal of Applied Physics, vol. 2, p. 312, ISSN: 0021-4922.
- Koráb, J.; Štefánik, P.; Kavecký, Š.; Šebo P. and Korb, G. (2002). *Thermal conductivity of unidirectional copper matrix carbon fibre composites*, Composites Part A: Applied Science and Manufacturing, vol. 33, 4, 2002, pp. 577-581, ISSN: 1359-835X.
- Kowbel, W. (2005). *Hybrid Al/SiC Composite Optics for IFE Applications*, Fusion Science and Technology, vol. 47, April 2005, pp. 596-600, ISSN: 1536-1055.
- Kim, K. T.; Cha, S. I.; Hong, S. H.; Hong, So. H. (2006), *Microstructures and tensile behavior of carbon nanotube reinforced Cu matrix nanocomposites*, Materials Science and Engineering A, vol. 430, pp. 27-33, ISSN: 0921-5093.
- Laha, T.; Chen, Y.; Lahiri, D. and Agarwal, A. (2009). *Tensile properties of carbon nanotube reinforced aluminum nanocomposite fabricated by plasma spray forming*, Composites Part A: Applied Science and Manufacturing, vol. 40, 5, pp. 589-594, ISSN: 1359-835X.
- Lan, J.; Yang, Y. and Li, X. (2004). *Microstructure and microhardness of SiC nanoparticles reinforced magnesium composites fabricated by ultrasonic method*, Materials Science and Engineering A, vol. 386, pp. 284-290, ISSN: 0921-5093.
- Lijie, C.; Zhenyu, R.; Jin-Phillipp N. Y. and Ruhle, M. (2006). *Investigation of the interfacial reaction between multi-walled carbon nanotubes and aluminum*, Acta Materialia, vol. 54, 20, pp. 5367-5375, ISSN: 1359-6454.

- Lim, D. K.; Shibayanag, T. and Gerlich, A. P. (2009). *Synthesis of multi-walled CNT reinforced aluminium alloy composite via friction stir processing*, Materials Science and Engineering A, vol. 507, pp. 194–199, ISSN: 0921-5093.
- Mamalis, A. G.; Vottea, I.; Manolakos, D. E.; Salay, A. and Desgardin G. (2001). *Chap. 37: On the Numerical Simulation of Shock Compacted mMetal Sheathed High-Tc superconducting billets* in Fundamental Issues and Applications of Shock-Wave and High-Strain Rate Phenomena, K. P. Staudhammer, L. E. Murr, and M. A. Meyers, (Eds.), Elsevier Science Ltd., Amsterdam pp. 289-295, ISBN: 008043896-2.
- Meyers, M. A.; Mishra, A. and Benson, D. J. (2006). *Mechanical properties of nanocrystalline materials*, Progress in Materials Science, vol. 51, pp. 427–556, ISSN: 0079-6425.
- Meyers, M. A. and Wang, S. L., (1988). *An Improved Method for Shock Consolidation of Powders*, Acta Materialia, vol. 36, 4, pp. 925-936, ISSN: 1359-6454.
- Meyyappan, M. (Ed.), (2004). *Carbon Nanotubes: Science and Applications*, CRC Press, ISBN 0-84932-111-5.
- Murr, Lawrence E. (Ed.), (1998). *Shock Waves for Industrial Applications*, Noyes Publishing, New York, pp. 237-472.
- Oelhafen, P. and Schuller, A. (2005). *Nanostructured materials for solar energy conversion*, Solar Energy, vol. 79, pp. 110–121, ISSN: 0038-092X.
- Peikrishvili, A. B.; Japaridze, L. A.; Staudhammer, K. P.; Marquis, F. S.; Chikhradze, N. M.; Gobejishvili, T. G. and Bantzuri, E. G. (2001). *Chap. 32: Explosive compaction of clad graphite powders and obtainig of coatings on their base* in Fundamental Issues and Applications of Shock-Wave and High-Strain Phenomena, K. P. Staudhammer, L. E. Murr, and M. A. Meyers(eds.), Elsevier Ltd, Amsterdam, p. 249, ISBN: 008043896-2.
- Probst, C.; Goujon, C., Gauvin, R. and Drew, R. A. L. (2005). *Enhanced wettability by copper electroless of coating of carbon nanotubes*, Advances in Ceramic Coatings and Ceramic-Metal Systems: A Collection of Papers Presented at the 29th International Conference on Advanced Ceramics and Composites, January 23-28, Cocoa Beach, Florida, Ceramic Engineering and Science Proceedings, vol. 26, 3, pp. 263-270, ISBN: 978-1-57498-233-6.
- Prummer, R and Kochsler, D. (2001) *Chap. 44 Bulk samples of intermetallics, obtained by explosive compaction* in Fundamental Issues and Applications of Shock-Wave and High-Strain Rate Phenomena, K. P. Staudhammer, L. E. Murr, and M. A. Meyers, (Eds.), Elsevier Science Ltd., Amsterdam, 2001, pp. 345-349, ISBN: 008043896-2.
- Prummer, R. A. and Ziegler, G. (1985). *Structure and annealing behavior of explosively compacted aluminum powders*, Powder Metallurgy International, vol. 9, 1, p. 1035, ISSN: 0048-5012.
- Prummer R. (2001), *Chap. 30: State or the art of explosive compaction* in Staudhammer K.P., Murr L. E., Meyers M. A., Editors. Fundamental Issues and Applications of Shock-Wave and High-Strain Rate Phenomena. Amsterdam: Elsevier Science Ltd.; pp. 235-244, ISBN: 008043896-2.
- Raghukandan, K.; Hokamoto, K.; Lee, J. S.; Chiba, A. and Pai, B. C., (2003). *An investigation on underwater shock consolidated carbon fiber reinforced Al composites*, Journal of Materials Processing Technology, vol. 134, pp. 329-337, ISSN: 0924-0136.
- Raming, T. P.; van Zyl, W. E.; Carton, E. P. and Verweij, H. (2004). *Sintering, sinterforging and explosive compaction to densify the dual phase nanocomposite system Y₂O₃-doped ZrO₂ and RuO₂*, Ceramics International, vol. 30, pp. 629–634, ISSN: 0272-8842.

- Rao, B. S.; Hemambar, Ch.; Pathak, A. V.; Patel, K. J.; Rödel, J. and Jayaram, V. (2006). *Al/SiC carriers for microwave integrated circuits by a new technique of pressureless infiltration*, IEEE Transactions on Electronics Packaging Manufacturing, January 2006, vol. 29, 1, pp. 58-63, ISSN:1521-334X.
- Rice, M. H.; Mcqueen, R. G. and Walsh, J. M. (1958). *Compression of solids by strong shock waves* in: F. Seitz, D. Turnbull (Eds.), *Solid State Physics*, No. VI F, Academic Press, New York.
- Rohatgi, P. K.; Schultz B. and Ferguson J. B., (2008), *Metal Matrix Nanocomposites for Structural Applications*, University of Wisconsin-Milwaukee Center for Composites, Milwaukee, WI.
- Sahin Y. and Acilar M., (2003). *Production and properties of SiCp-reinforced aluminium alloy composites*, Composites: Part A, v. 34, pp. 709-718, Composites Part A: Applied Science and Manufacturing, vol. 34, 8, pp. 709-718, ISSN: 1359-835X.
- Salas, W.; Alba-Baena, N. G. and Murr, L. E., (2007). *Explosive Shock-Wave Consolidation of Aluminum Powder/Carbon Nanotube Aggregate Mixtures: Optical and Electron Metallography*, Journal Metallurgical and Materials Transactions A, vol. 38, 12, ISSN: 1073-5623.
- Salvetat-Delmotte, J. and Rubio, A. (2002). *Mechanical properties of carbon nanotubes: a fiber digest for beginners*, Carbon, vol. 40, 10, pp. 1729-1734, ISSN: 0008-6223.
- Schwartz, M. M. (1997). *Composite Materials Handbook*, vol. 2, Prentice Hall, ISBN: 0133000397.
- Sherif El-Eskandarany, M. (1998). *Mechanical solid state mixing for synthesizing of SiC/Al nanocomposites*, Journal of Alloys and Compounds, vol. 279, pp. 263-271, ISSN: 0925-8388.
- Yoshiaki, Sh.; Toshiyasu, N. and Iwao, M. (1995). *Corrosion resistance of Al-based metal matrix composites*, Materials Science and Engineering A, vol. 198, 1-2, pp.113-118, ISSN: 0921-5093.
- SivaKumar, K.; Soloman, R.P.; Balakrishna, B. T. and Hokamoto, K. (2001). *Studies on Shock consolidated 2124 Al-40 vol.% SiCp composites*, Journal of Materials Processing Technology, vol. 115, pp. 396-401, ISSN: 0924-0136.
- SivaKumar, K.; Hokamoto, K.; Nakano, S. and Fijita, M. (2001). *Chap. 40 Fabrication of 2124 Al-SiC metal matrix composites by one dimensional underwater shock consolidation in Fundamental Issues and Applications of Shock-Wave and High-Strain Rate Phenomena*, K. P. Staudhammer, L.E. Murr, and M. A. Meyers, (Eds.), Elsevier Science Ltd., Amsterdam, pp. 313-320, ISBN: 008043896-2.
- Sivakumar, K.; Balakrishna, B. T. and Ramakrishnan, P. (1996). *Dynamic consolidation of aluminium and Al-20 V/o SiCp composite powders*, Journal of Materials Processing Technology, vol. 62, pp. 191-198, ISSN: 0924-0136.
- Stuivinga M.; Verbeek H. J. and Carton E. P. (1999). *The Double Explosive Layer Cylindrical Compaction Method*, Journal of Materials Processing Technology, vol. 85, pp. 115-120, ISSN: 0924-0136.
- Thadani, N. N. (1988). *Shock compression processing of powders*, Advanced Materials and Manufacturing Processes, vol. 3, 4, pp. 493-549, ISSN: 1042-6914.
- Thostenson, E. T.; Ren, Z. and Chou, T. W. (2001). *Advances in the science and technology of carbon nanotubes and their composites: a review*. Composites Science and Technology, vol. 61, pp. 1899-1912, ISSN: 0266-3538.

- Tjong S. C. and Ma, Z. Y. (1997). *The high-temperature creep behaviour of aluminium-matrix composites reinforced with SiC, Al₂O₃ and TiB₂ particles*, Composites Science and Technology, vol. 57, 6, pp. 697-702, ISSN: 0266-3538.
- Tong, W.; Ravichandrant, G.; Christman, T. and Vreeland Jr, T. (1995). *Processing SiC-particulate reinforced titanium-based metal matrix composites by shock wave consolidation*, Acta Metallurgica et Materialia, vol. 43, 1, pp. 235-250, ISSN: 1359-6454.
- Torralba, J. M.; da Costa, C. E. and Velasco, F. (2003). *P/M aluminum matrix composites: an overview*, Journal of Materials Processing Technology, vol. 133, pp. 203–206, ISSN: 0924-0136.
- Torquato, S., (2002). *Random Heterogeneous Materials: Microstructure and Macroscopic Properties*, Springer, ISBN: 0-387-95167-9.
- Vandersall, K. S. and Thadhani, N. N. (2001). *Chap. 34 Investigation of shock-induced chemical reactions in Mo-Si powder mixtures* in Fundamental Issues and Applications of Shock-Wave and High-Strain Rate Phenomena, K.P. Staudhammer, L.E. Murr, and M. A. Meyers, (Eds.), Elsevier Science Ltd., Amsterdam, pp. 267-274, ISBN: 008043896-2.
- Wang, L.; Jiang, W. and Chen, L. (2004). *Fabrication and characterization of nano-SiC particles reinforced TiC/SiC nano composites*, Materials Letters, vol. 58, pp. 1401–1404, ISSN: 0167-577X.
- Wang, H. Z.; Wu, S. Q. and Tjong, S. C. (1996). *Mechanical and wear behavior of an Al/Si alloy metal-matrix composite reinforced with aluminosilicate fiber*, Composites Science and Technology, vol. 56, 11, pp. 1261-1270, ISSN: 0266-3538.
- Wang, X.; Wu, G.; Sun, D.; Qin, Ch. and Tian, Y. (2004). *Micro-yield property of sub-micron Al₂O₃ particle reinforced 2024 aluminum matrix composite*, Materials Letters, vol. 58, pp. 333– 336, ISSN: 0167-577X.
- Ward, P. J.; Atkinson, H. V.; Anderson, P. R. G.; Elias, L. G.; Garcia, B.; Kahlen L. and Rodriguez-Ibabe, J.M. (1996). *Semi-solid processing of novel MMCs based on hypereutectic aluminium-silicon alloys*, Acta Materialia, vol. 44, 5, pp. 1717-1727, ISSN: 1359-6454.
- Weimar, P. and Pruemmer, R. (2001). *Chap. 36 Explosive compaction of nanocrystalline alumina powder* in Fundamental Issues and Applications of Shock-Wave and High-Strain Rate Phenomena, K.P. Staudhammer, L.E. Murr, and M. A. Meyers, (Eds.), Elsevier Science, Ltd., Amsterdam, pp. 283-287, ISBN: 008043896-2.
- Withers, G. (2005). *ULTALITE Aluminum Composites*, Advanced Materials & Processes, September, pp. 44-48, ISSN: 0882-7958.
- Xu, C. L.; Wei, B. Q.; Ma, R. Z.; Liang, J.; Ma, X. K. and Wu D. H. (1999). *Fabrication of aluminum-carbon nanotube composites and their electrical properties*, Carbon, vol. 37, 5, pp. 855-858, ISSN: 0008-6223.
- Yang, Y.; Lan, J. and Li, X. (2004). *Study on bulk aluminum matrix nano-composite fabricated by ultrasonic dispersion of nano-sized SiC particles in molten aluminum alloy*, Materials Science and Engineering A, vol. 380, pp. 378–383, ISSN: 0921-5093.
- Zhong, R.; Cong, H. and Hou, P. (2004). *Fabrication of nano-Al based composites reinforced by single-walled carbon nanotubes*, Carbon, vol. 41, 4, pp. 848–851, ISSN: 0008-6223.



Carbon Nanotubes

Edited by Jose Mauricio Marulanda

ISBN 978-953-307-054-4

Hard cover, 766 pages

Publisher InTech

Published online 01, March, 2010

Published in print edition March, 2010

This book has been outlined as follows: A review on the literature and increasing research interests in the field of carbon nanotubes. Fabrication techniques followed by an analysis on the physical properties of carbon nanotubes. The device physics of implemented carbon nanotubes applications along with proposed models in an effort to describe their behavior in circuits and interconnects. And ultimately, the book pursues a significant amount of work in applications of carbon nanotubes in sensors, nanoparticles and nanostructures, and biotechnology. Readers of this book should have a strong background on physical electronics and semiconductor device physics. Philanthropists and readers with strong background in quantum transport physics and semiconductors materials could definitely benefit from the results presented in the chapters of this book. Especially, those with research interests in the areas of nanoparticles and nanotechnology.

How to reference

In order to correctly reference this scholarly work, feel free to copy and paste the following:

Noe Alba-Baena, Wazne Salas and Lawrence E. Murr (2010). Shock-Wave-Compaction (SWC) of Al/CNT Two Phase Systems, Carbon Nanotubes, Jose Mauricio Marulanda (Ed.), ISBN: 978-953-307-054-4, InTech, Available from: <http://www.intechopen.com/books/carbon-nanotubes/shock-wave-compaction-swc-of-al-cnt-two-phase-systems>

INTECH
open science | open minds

InTech Europe

University Campus STeP Ri
Slavka Krautzeka 83/A
51000 Rijeka, Croatia
Phone: +385 (51) 770 447
Fax: +385 (51) 686 166
www.intechopen.com

InTech China

Unit 405, Office Block, Hotel Equatorial Shanghai
No.65, Yan An Road (West), Shanghai, 200040, China
中国上海市延安西路65号上海国际贵都大饭店办公楼405单元
Phone: +86-21-62489820
Fax: +86-21-62489821

© 2010 The Author(s). Licensee IntechOpen. This chapter is distributed under the terms of the [Creative Commons Attribution-NonCommercial-ShareAlike-3.0 License](https://creativecommons.org/licenses/by-nc-sa/3.0/), which permits use, distribution and reproduction for non-commercial purposes, provided the original is properly cited and derivative works building on this content are distributed under the same license.

IntechOpen

IntechOpen